© 2015. Published by The Company of Biologists Ltd | Development (2015) 142, 1516-1527 doi:10.1242/dev.119065

RESEARCH ARTICLE

Wnt5a and *Wnt11* regulate mammalian anterior-posterior axis elongation

Philipp Andre[1], Hai Song[1,*], Wantae Kim[1], Andreas Kispert[2] and Yingzi Yang[1,3,‡]

ABSTRACT

Mesoderm formation and subsequent anterior-posterior (A-P) axis elongation are fundamental aspects of gastrulation, which is initiated by formation of the primitive streak (PS). Convergent extension (CE) movements and epithelial-mesenchymal transition (EMT) are important for A-P axis elongation in vertebrate embryos. The evolutionarily conserved planar cell polarity (PCP) pathway regulates CE, and Wnts regulate many aspects of gastrulation including CE and EMT. However, the Wnt ligands that regulate A-P axis elongation in mammalian development remain unknown. *Wnt11* and *Wnt5a* regulate axis elongation in lower vertebrates, but only *Wnt5a*, not *Wnt11*, regulates mammalian PCP signaling and A-P axis elongation in development. Here, by generating *Wnt5a; Wnt11* compound mutants, we show that *Wnt11* and *Wnt5a* play redundant roles during mouse A-P axis elongation. Both genes regulate trunk notochord extension through PCP-controlled CE of notochord cells, establishing a role for *Wnt11* in mammalian PCP. We show that *Wnt5a* and *Wnt11* are required for proper patterning of the neural tube and somites by regulating notochord formation, and provide evidence that both genes are required for the generation and migration of axial and paraxial mesodermal precursor cells by regulating EMT. Axial and paraxial mesodermal precursors ectopically accumulate in the PS at late gastrula stages in $Wnt5a^{-/-}; Wnt11^{-/-}$ embryos and these cells ectopically express epithelial cell adhesion molecules. Our data suggest that *Wnt5a* and *Wnt11* regulate EMT by inducing p38 (Mapk14) phosphorylation. Our findings provide new insights into the role of *Wnt5a* and *Wnt11* in mouse early development and also in cancer metastasis, during which EMT plays a crucial role.

KEY WORDS: Convergent extension, EMT, Gastrulation, Notochord, Planar cell polarity, Wnt

INTRODUCTION

In vertebrate embryos, the basic body plan is established during gastrulation through the formation of three germ layers and a major rearrangement of cells. Gastrulation is initiated with primitive streak (PS) formation at the posterior of the embryo (Tam and Behringer, 1997). The PS elongates anteriorly during gastrulation. Within the PS, cells of the primitive ectoderm delaminate and undergo an epithelial-mesenchymal transition (EMT) (Arnold and Robertson, 2009) to give rise to mesodermal and endodermal structures (Beddington and Robertson, 1999; Tam and Loebel, 2007). Defective EMT results in severe phenotypes, as cells fail to migrate away from the PS and instead accumulate (Sun et al., 1999; Ciruna and Rossant, 2001). Besides its essential role in gastrulation, EMT is also crucial for other developmental processes, wound healing, fibrosis and cancer metastasis (Thiery et al., 2009). However, the molecular mechanisms that regulate EMT remain to be fully elucidated.

Anterior-posterior (A-P) body axis elongation requires continuous generation and proper organization of axial and paraxial mesoderm. Fate-mapping studies have revealed that cells emerging from the anterior PS give rise to the axial mesoderm that forms the notochord (Lawson et al., 1991). The notochord serves as an important signaling center that patterns the overlying neuroectoderm and adjacent somites through secretion of signaling molecules such as sonic hedgehog (Shh) (Echelard et al., 1993; Chiang et al., 1996; reviewed by Cleaver and Krieg, 2001). Anterior to the PS, an indentation called the posterior notochord (PNC, also referred to as the node or ventral node) forms at mid-gastrula stages (Blum et al., 2007). The PNC provides instructive signals during mouse left-right determination and is continuous with the notochord (Sulik et al., 1994; Nonaka et al., 2002). Cells of the trunk and tail notochord are derived from the PNC (Sulik et al., 1994; Yamanaka et al., 2007; Ukita et al., 2009). However, since PNC cells are ciliated and proliferate at a very low rate, a region consisting of the anteriormost streak and the posteriormost part of the node/PNC, called the node/streak border (NSB), is considered the origin of notochord precursors (Sulik et al., 1994; Bellomo et al., 1996; Cambray and Wilson, 2002, 2007; Ukita et al., 2009). PNC cells express *Noto* and the epithelial marker E-cadherin (Abdelkhalek et al., 2004; Plouhinec et al., 2004; Yamanaka et al., 2007). Genetic fate-mapping studies revealed that the *Noto*-expressing cells in the PNC contribute to notochord precursor cells (NPCs) that form the trunk and tail notochord as well as some of the paraxial mesoderm (Yamanaka et al., 2007; Ukita et al., 2009). In addition, paraxial mesodermal cells are derived from more posterior regions of the PS and migrate anteriorly to give rise to the somites (Tam and Beddington, 1987; Tam et al., 2000).

The trunk notochord is derived from the PNC and forms by convergent extension (CE) (Sausedo and Schoenwolf, 1994; Ybot-Gonzalez et al., 2007), whereas the tail notochord (posterior notochord extension) is generated by peripheral PNC cells actively migrating posteriorly (Sulik et al., 1994; Yamanaka et al., 2007). Although continuous production of notochord cells by the NPCs is crucial to establish the correct body plan (Ukita et al., 2009), the molecular and cellular regulation of NPC generation remains unknown. The Wnt signaling pathways regulate many fundamentally important developmental processes, including gastrulation. Although Wnts can signal through the canonical pathway mediated by β-catenin, the β-catenin-independent Wnt/planar cell polarity (PCP) pathway has recently emerged as a regulator of many key processes (Song et al., 2010; Gao et al.,

[1]Genetic Disease Research Branch, National Human Genome Research Institute, Bethesda, MD 20814, USA. [2]Institut für Molekularbiologie, Medizinische Hochschule Hannover, Hannover D-30625, Germany. [3]Department of Developmental Biology, Harvard School of Dental Medicine, 188 Longwood Ave., Boston, MA 02115, USA.
*Present address: Life Sciences Institute, Zhejiang University, 866 Yuhangtang Road, Hangzhou, Zhejiang Province 310058, People's Republic of China.

‡Author for correspondence (yingzi_yang@hsdm.harvard.edu)

Received 24 October 2014; Accepted 4 March 2015

Development (2015) 142, 1516-1527 doi:10.1242/dev.119065

2011). The PCP pathway was initially identified in *Drosophila melanogaster*, where it controls the establishment of a polarity within an epithelial sheet perpendicular to apical-basal polarity. A group of core PCP components has been identified in *Drosophila*, and these are functionally conserved in vertebrates (Tree et al., 2002; Seifert and Mlodzik, 2007; McNeill, 2010). In vertebrates, PCP regulates CE of axial and paraxial mesodermal cells during axis elongation, and defects in PCP signaling result in a shortened and widened A-P axis (Greene et al., 1998; Keller, 2002; Wallingford et al., 2002; Ybot-Gonzalez et al., 2007; Roszko et al., 2009; Song et al., 2010; Mahaffey et al., 2013). CE movements are characterized by polarized cell behavior as cells converge along one axis, intercalate and finally extend along the axis perpendicular to the initial cell movements (Keller, 2002). In mammals, PCP signaling is essential for many morphological processes, including closure of the neural tube, inner ear hair cell polarity, left-right asymmetry and elongation of the A-P axis (Kibar et al., 2001; Curtin et al., 2003; Montcouquiol et al., 2003; Wang et al., 2006; Ybot-Gonzalez et al., 2007; Borovina et al., 2010; Hashimoto et al., 2010; Song et al., 2010; Gao et al., 2011). Mutations in human core PCP components cause congenital neural tube defects (NTDs) such as spina bifida (Kibar et al., 2007; Lei et al., 2010). However, despite the importance of PCP signaling, the mechanism underlying Wnt regulation of PCP signaling is poorly understood.

Wnt5a and *Wnt11* have been shown to regulate vertebrate PCP signaling. Loss of *Wnt5a* results in a severe shortening of the A-P axis and limb truncations (Yamaguchi et al., 1999a). Wnt5a regulates PCP establishment by inducing phosphorylation of Vangl2, a core PCP protein (Gao et al., 2011). In *Xenopus* embryos, expression of a dominant-negative Wnt11 results in NTDs and CE defects (Tada and Smith, 2000) and the zebrafish *wnt11* mutant *silberblick* exhibits CE defects in the developing notochord that result in a shortened A-P axis (Heisenberg et al., 2000). However, mouse *Wnt11*$^{-/-}$ embryos do not show PCP defects, in contrast to the *silberblick* mutant (Majumdar et al., 2003), raising the question of whether *Wnt11* regulates PCP signaling in mammals.

Here we show that, upon loss of both *Wnt5a* and *Wnt11*, the phenotype of *Wnt5a*$^{-/-}$ embryos is exacerbated as the A-P axis is further shortened, indicating functional redundancy of these two signaling molecules during axis formation in the murine embryo. We further show that *Wnt5a* and *Wnt11* regulate CE, EMT and cell migration, disruption of which results in defects in notochord formation and in patterning of the neural tube and somites.

RESULTS

Wnt5a and *Wnt11* are required for PCP during CE of notochord cells

wnt11 is required to regulate axis elongation through PCP in zebrafish (Heisenberg et al., 2000). The lack of similar defects in mouse *Wnt11* mutants (Majumdar et al., 2003) suggests that *Wnt11* might play redundant roles with *Wnt5a* during mouse gastrulation. We first examined the expression of *Wnt5a* and *Wnt11* in early mouse embryos and confirmed that *Wnt5a* is expressed in a caudal-to-rostral gradient in the PS (supplementary material Fig. S1A-D) (Yamaguchi et al., 1999a), whereas *Wnt11* expression is more restricted (supplementary material Fig. S1E-H) (Kispert et al., 1996). *Wnt11* was expressed in the PNC and in the forming heart, as previously reported (Kispert et al., 1996). To investigate a possible redundancy between *Wnt5a* and *Wnt11* during early embryonic development, we generated *Wnt5a; Wnt11* double-mutant mouse embryos. *Wnt5a*$^{-/-}$*; Wnt11*$^{-/-}$ embryos were found at the expected Mendelian ratio between E8.5 and E10.5 (Fig. 1A-L), and died between E10.5 and E11.5. The phenotype of *Wnt5a*$^{-/-}$*; Wnt11*$^{-/-}$ embryos became apparent at ∼E8.5 (Fig. 1A-D) and was much more severe than that of the *Wnt5a* single mutant, as the A-P axis was further shortened (Fig. 1G,H,K,L). Therefore, *Wnt11* plays redundant roles with *Wnt5a* in regulating early mouse embryonic development. There was no difference between *Wnt5a*$^{-/-}$*; Wnt11*$^{+/-}$ and *Wnt5a*$^{-/-}$ embryos in terms of morphology and marker gene expression (data not shown).

A-P axis elongation is driven by PCP-mediated CE movements within the notochord and paraxial mesoderm. Defects in PCP signaling result in a shortened and widened A-P axis (Ybot-Gonzalez et al., 2007; Song et al., 2010). To test whether similar defects were caused by loss of *Wnt5a* and *Wnt11*, we examined the length/width ratio at E8.5. *Wnt5a*$^{-/-}$*; Wnt11*$^{+/-}$ embryos displayed a decrease in the length/width ratio, which was enhanced in *Wnt5a*$^{-/-}$*; Wnt11*$^{-/-}$ mutants (supplementary material Fig. S2A-D). Next, we investigated the expression of *Shh*, which marks the notochord and floor plate at E9.5 (Echelard et al., 1993), to assess notochord formation (Fig. 1M-P). Surprisingly, the notochord was not only reduced in length but also in width in *Wnt5a*$^{-/-}$*; Wnt11*$^{-/-}$ embryos (Fig. 1M′-P′). To further understand the observed notochord malformation, we investigated expression of the transcription factor brachyury (*T*), a marker of the nascent mesoderm and the notochord (Wilson et al., 1995). At E8.0, we found a sparse and irregular *T* expression pattern, and fewer cells expressed *T* in *Wnt5a*$^{-/-}$*; Wnt11*$^{-/-}$ than in control embryos (Fig. 2A,B).

To test whether the reduction in notochord length in *Wnt5a*$^{-/-}$*; Wnt11*$^{-/-}$ embryos was due to defective CE, we performed *in vitro* DiI labeling experiments to trace cells of the PNC. After 12 h of *in vitro* culture, most labeled PNC cells had migrated anteriorly along the midline in the control (Fig. 2C,C′; *n*=27/33). However, in *Wnt5a*$^{-/-}$*; Wnt11*$^{-/-}$ embryos, the labeled PNC cells lacked directionality and migrated in more random directions (Fig. 2D,D′; *n*=5/6). Thus, the distance of migration away from the initial labeling position (PNC) was shorter. To confirm that notochord cells had been successfully labeled by DiI injections, we sectioned the labeled embryos and found that T-positive cells were labeled by DiI (supplementary material Fig. S3A-D). Additionally, we observed labeled cells in the paraxial mesoderm (Fig. 2C,D; supplementary material Fig. S3C,D). Taken together, these results show that *Wnt5a* and *Wnt11* are required for proper CE of notochord and paraxial mesoderm cells.

During lengthening of the notochord along the A-P axis, the cells in the axial midline elongate along the mediolateral axis and intercalate to form two adjacent rows of notochord cells. This is typical of highly conserved CE movements. The PCP pathway has been shown to be instructive for the correct alignment of notochord cells during CE and is regulated by *Wnt5a* (Qian et al., 2007; Ybot-Gonzalez et al., 2007; Gao et al., 2011). Therefore, we tested whether notochord cells exhibit asymmetric localization of the core PCP protein Vangl1, as the asymmetric localization of core PCP proteins is a hallmark of PCP signaling (Klein and Mlodzik, 2005; Song et al., 2010). In control embryos, in many notochord cells, as marked by T expression, Vangl1 was localized asymmetrically with an increase on cell membranes perpendicular to the A-P axis as compared with the parallel axis. Additionally, the notochord cells were elongated mediolaterally (Fig. 2E,E′). By contrast, in *Wnt5a*$^{-/-}$*; Wnt11*$^{-/-}$ embryos, Vangl1 protein levels were much reduced. Very few cells showed asymmetrically localized Vangl1 and the cells were less elongated, with irregular morphology (Fig. 2F,F′). These results

Development (2015) 142, 1516-1527 doi:10.1242/dev.119065

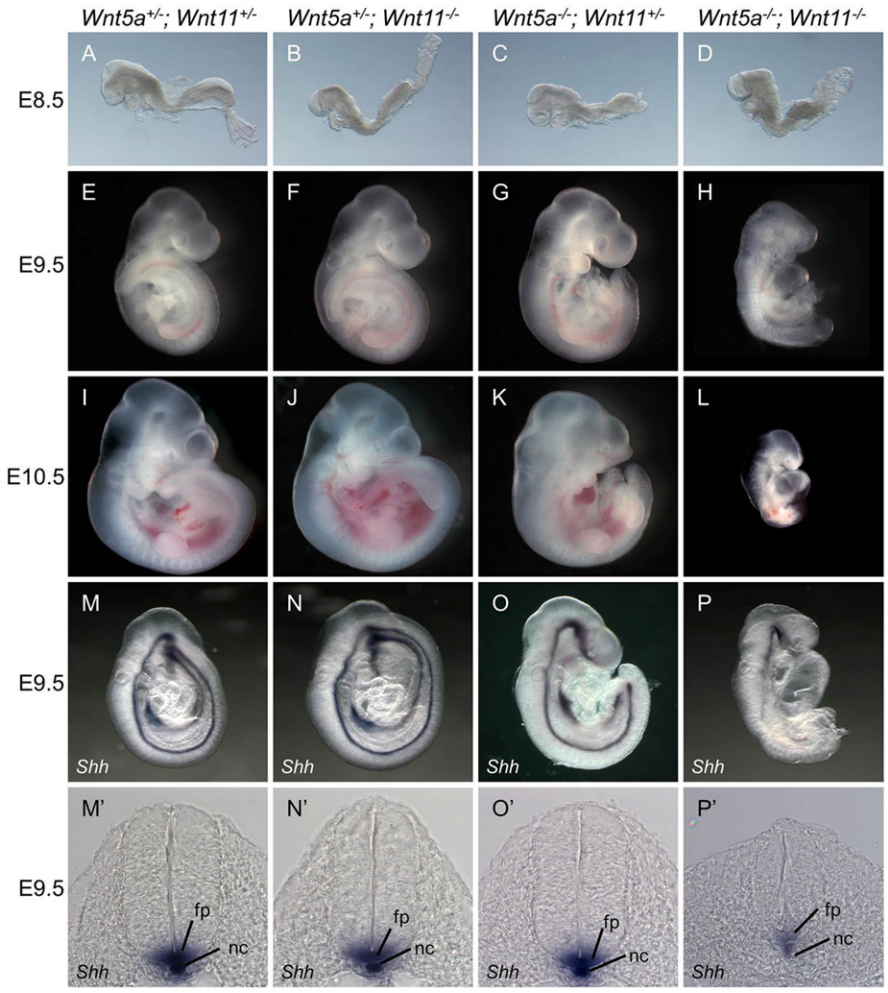

Fig. 1. A-P axis and notochord defects in *Wnt5a*$^{-/-}$; *Wnt11*$^{-/-}$ embryos. (A-L) Phenotypic analysis of mouse embryos of the indicated genotypes at the stages shown reveals severe shortening of the A-P axis in *Wnt5a*$^{-/-}$; *Wnt11*$^{-/-}$ (D,H,L) as compared with *Wnt5a*$^{-/-}$; *Wnt11*$^{+/-}$ (C,G,K) embryos. (M-P) Whole-mount *in situ* hybridization for the notochord and floor plate marker *Shh*. (M′-P′) Transverse sections of the embryos shown in M-P at the forelimb bud level. fp, floor plate; nc, notochord.

indicate that PCP signaling, and hence CE regulated by PCP, is reduced in the absence of *Wnt5a* and *Wnt11*.

The early heart tube of the *Wnt5a*$^{-/-}$; *Wnt11*$^{-/-}$embryo failed to undergo normal rightward looping and remained as a linear tube at E9.5 (Fig. 3A-C). This malformation may lead to embryonic lethality and confirmed the findings of a recent study (Cohen et al., 2012). *Nkx2.5*, a homeobox transcriptional regulator that is essential for heart looping (Lyons et al., 1995), was expressed throughout the myocardial layer of the heart tube in control embryos at E9.5 (Fig. 3A). Normal *Nkx2.5* expression was maintained in the heart tube of *Wnt5a*$^{-/-}$; *Wnt11*$^{-/-}$ embryos at E9.5 (Fig. 3C), raising the question of whether laterality determination is affected by loss of *Wnt5a* and *Wnt11*. We have previously shown that PCP breaks bilateral symmetry by positioning cilia to the posterior side of the PNC cells (Nonaka et al., 2005; Song et al., 2010), and in *Xenopus* embryos knocking down *Wnt11b* results in left-right defects

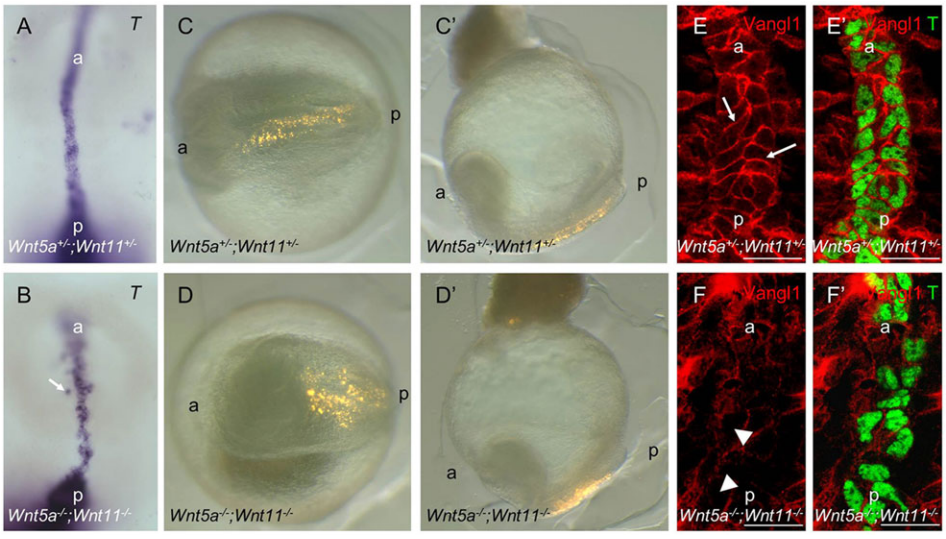

Fig. 2. Defective CE and PCP signaling in the notochord of *Wnt5a*$^{-/-}$; *Wnt11*$^{-/-}$ embryos. (A,B) Whole-mount *in situ* hybridization for brachyury (*T*) in ventral views of the notochord at E8.5. *T* expression outside of the notochord is indicated by an arrow in B. (C-D′) DiI labeling of PNC cells. Ventral (C,D) and distal (C′,D′) views of the embryos 12 h after labeling. (E,F) Vangl1 expression as shown by immunofluorescence in notochord cells of E8.5 embryos. Asymmetric localization of Vangl1 protein along the A-P axis is indicated by arrows in E. Cells with irregular morphology are indicated by arrowheads in F. (E′,F′) Co-staining of Vangl1 (red) and T (green) in notochord cells at E8.5. a, anterior; p, posterior. Scale bars: 25 µm in E-F′.

Development (2015) 142, 1516-1527 doi:10.1242/dev.119065

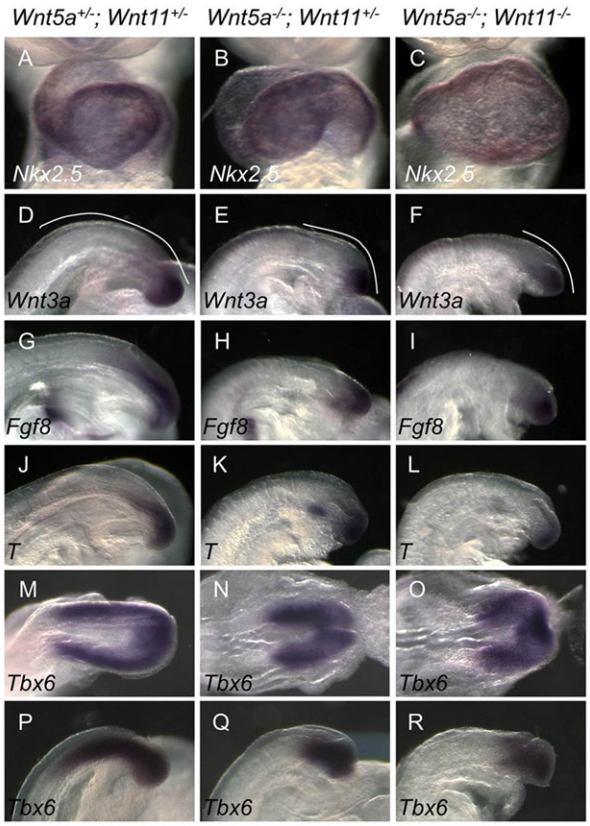

Fig. 3. *Wnt5a*$^{-/-}$; *Wnt11*$^{-/-}$ embryos display malformed heart and tail bud. (A-C) Heart formation is shown by whole-mount *in situ* hybridization for *Nkx2.5* in E9.5 embryos. *Wnt5a*$^{-/-}$; *Wnt11*$^{-/-}$ embryos fail to undergo heart looping. (D-L) Expression of *Wnt3a* (D-F), *Fgf8* (G-I) and *T* (J-L) in the tail buds of E9.5 embryos as shown by whole-mount *in situ* hybridization. The line in D-F indicates extension of unsegmented mesoderm. (M-R) Expression of *Tbx6* in the posterior of embryos at E8.5 in dorsal view (M-O) and in tail buds of E9.5 embryos (P-R).

(Walentek et al., 2013). In order to test whether *Wnt5a* and *Wnt11* control PCP-regulated laterality determination, we examined asymmetric gene expression of *Nodal* and *Pitx2* (Lowe et al., 1996; Logan et al., 1998). We observed normal, left-sided expression of *Nodal* and *Pitx2* in nine out of ten *Wnt5a*$^{-/-}$; *Wnt11*$^{-/-}$ embryos, with only one embryo showing an inverted, right-sided *Nodal* expression (supplementary material Fig. S4A-C; data not shown). Furthermore, we were able to detect asymmetric localization of Vangl1 in the PNC cells of *Wnt5a*$^{-/-}$; *Wnt11*$^{-/-}$ embryos (supplementary material Fig. S4D,E). Thus, the absence of Wnt5a and Wnt11 signaling resulted in left-right patterning defects only at very low penetrance. These results suggest that other Wnt ligands expressed in the PS might compensate for the loss of *Wnt5a* and *Wnt11* during laterality determination. Our data indicate that the observed heart-looping defect occurs further downstream in development and is not regulated by laterality determination in this case.

Our analysis of notochord formation and *Shh* expression in the *Wnt5a*$^{-/-}$; *Wnt11*$^{-/-}$ embryos suggests that the reduction in notochord size resulted in a smaller floor plate, as *Shh* expressed in the notochord induces floor plate formation (Echelard et al., 1993; Placzek et al., 1993). Since Shh secreted from the notochord and the floor plate is required for repression of dorsal and induction of ventral cell fates in the neural tube (NT) (Echelard et al., 1993; Chiang et al., 1996), we tested whether the reduction of *Shh* expression in *Wnt5a*$^{-/-}$; *Wnt11*$^{-/-}$ embryos resulted in a dorsalized NT. Indeed, expression of *Pax6*, which is a dorsal NT marker repressed by Shh (Ericson et al., 1997), was expanded ventrally in the *Wnt5a*$^{-/-}$; *Wnt11*$^{-/-}$ embryos (supplementary material Fig. S5A-C). Conversely, expression of the ventral markers Nkx2.2, Olig2 and Nkx6.1, which depend on Shh induction (Chiang et al., 1996), was reduced in the *Wnt5a*$^{-/-}$; *Wnt11*$^{-/-}$ mutants (supplementary material Fig. S5D-L). To exclude the possibility that the reduction in ventral cells was the result of a reduced number of cells in the NT, we quantified the ratio of labeled to unlabeled NT cells and were able to confirm a dorsalized NT in the *Wnt5a*$^{-/-}$; *Wnt11*$^{-/-}$ embryos (supplementary material Fig. S5M).

Somitogenesis depends on proper *Wnt5a* and *Wnt11* signaling

Apart from a shortened A-P axis, we also observed smaller and irregular somites in *Wnt5a*$^{-/-}$; *Wnt11*$^{-/-}$ embryos, indicating defects in somite formation. In addition, the A-P axis reduction in *Wnt5a*$^{-/-}$; *Wnt11*$^{-/-}$ embryos was most severe in posterior regions, where cells of the PS and later the tailbud give rise to the paraxial mesoderm, the precursor of the somites (Tam and Beddington, 1987; Tam et al., 2000). To understand the defects in somitogenesis in the absence of *Wnt5a* and *Wnt11*, we first investigated the expression of *Wnt3a* and *Fgf8*, which are essential for the formation of paraxial mesoderm (Takada et al., 1994; Crossley and Martin, 1995). The expression levels of *Wnt3a* and *Fgf8* were similar in all investigated specimens (Fig. 3D-I). Furthermore, Wnt/β-catenin signaling indicated by TOPGAL (DasGupta and Fuchs, 1999) and Fgf signaling indicated by *Spry4* expression (Minowada et al., 1999) were normal in *Wnt5a*$^{-/-}$; *Wnt11*$^{-/-}$ embryos (supplementary material Fig. S6A-F). However, the expression domains of *Wnt3a* and *Fgf8* were significantly shortened along the A-P axis in *Wnt5a*$^{-/-}$; *Wnt11*$^{-/-}$ as compared with control and *Wnt5a*$^{-/-}$; *Wnt11*$^{+/-}$ embryos (Fig. 3D-I).

This shortening might result from a reduction in paraxial mesoderm formation and/or defects in mesodermal cell migration. Mesodermal movements are controlled by *T*, which is expressed in the PS (Wilson et al., 1995). In the absence of *Wnt5a* and *Wnt11*, we observed a reduction of *T* expression as compared with the *Wnt5*$^{-/-}$ mutant, indicating defects in mesoderm formation and migration (Fig. 3J-L). To investigate paraxial mesoderm formation we compared the expression of *Tbx6* at E8.5 and E9.5 (Fig. 3M-R) (Chapman and Papaioannou, 1998). In the *Wnt5a*$^{-/-}$; *Wnt11*$^{+/-}$ embryos, the *Tbx6* expression domain was reduced, and this was further enhanced in *Wnt5a*$^{-/-}$; *Wnt11*$^{-/-}$ embryos at E8.5 (Fig. 3N,O). Additionally, there was a reduced level of *Tbx6* expression at E9.5 (Fig. 3Q,R), suggesting defects in paraxial mesoderm formation in the absence of *Wnt5a* and *Wnt11*.

Our results indicated that the defects in somitogenesis were not due to abnormal Wnt3a and Fgf signaling. As *Wnt5a* has been suggested to regulate the proliferation of paraxial mesoderm cells (Yamaguchi et al., 1999a), we examined cell proliferation and survival in the paraxial mesoderm by anti-phospho-histone H3 (PHP3) antibody staining and TUNEL assay, respectively. At E8.5, no significant difference in cell proliferation or survival was observed in *Wnt5a*$^{-/-}$; *Wnt11*$^{-/-}$ and control embryos (supplementary material Fig. S7A-F). At E9.5, cell death was significantly increased in the *Wnt5a*$^{-/-}$; *Wnt11*$^{-/-}$ embryos, especially in the tail bud (supplementary material Fig. S7G-I), and proliferation in the paraxial mesoderm of *Wnt5a*$^{-/-}$; *Wnt11*$^{-/-}$ embryos was slightly reduced (supplementary material Fig. S7J-L). At E10.5, a substantial increase in cell death and almost no cell proliferation were detected in *Wnt5a*$^{-/-}$; *Wnt11*$^{-/-}$ embryos (supplementary material Fig. S7M-R). These results indicate that

Development (2015) 142, 1516-1527 doi:10.1242/dev.119065

Wnt5a and *Wnt11* promote cell proliferation and survival independently of Wnt3a and Fgf signaling in the paraxial mesoderm.

In *Wnt5a*$^{-/-}$; *Wnt11*$^{-/-}$ embryos the somites were not only smaller but also irregular, suggesting that, apart from the defects in cell proliferation and survival, somite patterning was also disrupted. To test this, we examined the expression of *Uncx4.1* (also known as *Uncx*), which marks the posterior compartment of mature somites (Mansouri et al., 1997). *Uncx4.1* was only expressed in the caudal part of somites in control embryos (Fig. 4A). However, *Uncx4.1* expression became continuous and sometimes asymmetric on the left and right side in the newly formed somites of *Wnt5a*$^{-/-}$; *Wnt11*$^{-/-}$ embryos (*n*=3/6; Fig. 4C). These results suggest that the periodic and synchronized segmentation of the paraxial mesoderm and the A-P polarity of the somite were disrupted in the absence of *Wnt5a* and *Wnt11*.

As Notch signaling plays fundamental roles in the formation and patterning of somites (Conlon et al., 1995; Kageyama et al., 2007), we examined Notch signaling in *Wnt5a*$^{-/-}$; *Wnt11*$^{-/-}$ embryos. *Mesp2* acts downstream of Notch signaling to specify the rostral compartments of somites and its expression is restricted to the future rostral somitic half (Saga et al., 1997). *Mesp2* expression was greatly reduced in *Wnt5a*$^{-/-}$; *Wnt11*$^{-/-}$ but not in *Wnt5a*$^{-/-}$; *Wnt11*$^{+/-}$ embryos (Fig. 4D-F). In addition, expression of *Hes7* and *Lfng*, which are Notch signaling effectors (Bessho et al., 2001; Dale et al., 2003), was also significantly diminished in *Wnt5a*$^{-/-}$; *Wnt11*$^{-/-}$ embryos (Fig. 4G-L), indicating that Notch signaling activity was reduced in the absence of *Wnt5a* and *Wnt11*. The expression of *Notch1* and *Notch2* was greatly reduced in the paraxial mesoderm of *Wnt5a*$^{-/-}$; *Wnt11*$^{-/-}$ embryos (Fig. 4M-R). However, the expression levels of the Notch ligands *Dll1* and *Dll3* were normal in the paraxial mesoderm of *Wnt5a*$^{-/-}$; *Wnt11*$^{-/-}$ embryos (Bettenhausen et al., 1995; Dunwoodie et al., 1997) (Fig. 4S-X). These results suggest that the reduced Notch signaling activity is likely to be due to diminished expression of *Notch1* and *Notch2* in the *Wnt5a*$^{-/-}$; *Wnt11*$^{-/-}$ embryos.

Consistent with the asymmetric expression pattern of *Uncx4.1* (Fig. 4C), we observed lateral asymmetric expression patterns of *Mesp2* and *Lfng* in *Wnt5a*$^{-/-}$; *Wnt11*$^{-/-}$ embryos (Fig. 4F,L), indicating defects in somite synchronization. As retinoic acid (RA) signaling is required for the bilateral symmetry of somite formation and establishment of the determination front (Vermot et al., 2005; Vermot and Pourquie, 2005; Sirbu and Duester, 2006), we examined the expression of *Raldh2* (*Aldh1a2*), the RA biosynthetic enzyme, and of *Cyp26b1*, the RA degrading enzyme (Zhao et al., 1996; White et al., 2000). *Raldh2* was expressed in the segmented region of the control embryos and its expression was reduced in the somites of *Wnt5a*$^{-/-}$; *Wnt11*$^{-/-}$ embryos at E9.5 (supplementary material Fig. S8A-C), whereas *Cyp26b1* expression in the tail bud remained normal (supplementary material Fig. S8D-F). Taken together, these results indicate that significantly reduced Notch and RA signaling inhibit proper somite formation in *Wnt5a*$^{-/-}$; *Wnt11*$^{-/-}$ embryos.

Wnt5a and *Wnt11* regulate EMT during late gastrula stages

The thinner notochord and smaller somites in *Wnt5a*$^{-/-}$; *Wnt11*$^{-/-}$ embryos prompted us to further investigate the molecular and cellular mechanisms underlying the defects in notochord and somite formation, focusing on posterior mesoderm formation and migration during gastrulation. Interestingly, we noticed an ectopic accumulation of cells in the *Wnt5a*$^{-/-}$; *Wnt11*$^{-/-}$ embryos at the posterior of the PNC at E8.5 (Fig. 5A-B′), suggesting that *Wnt5a* and *Wnt11* are additionally required for the specification and/or migration of mesodermal cells. We speculated that this ectopic cell

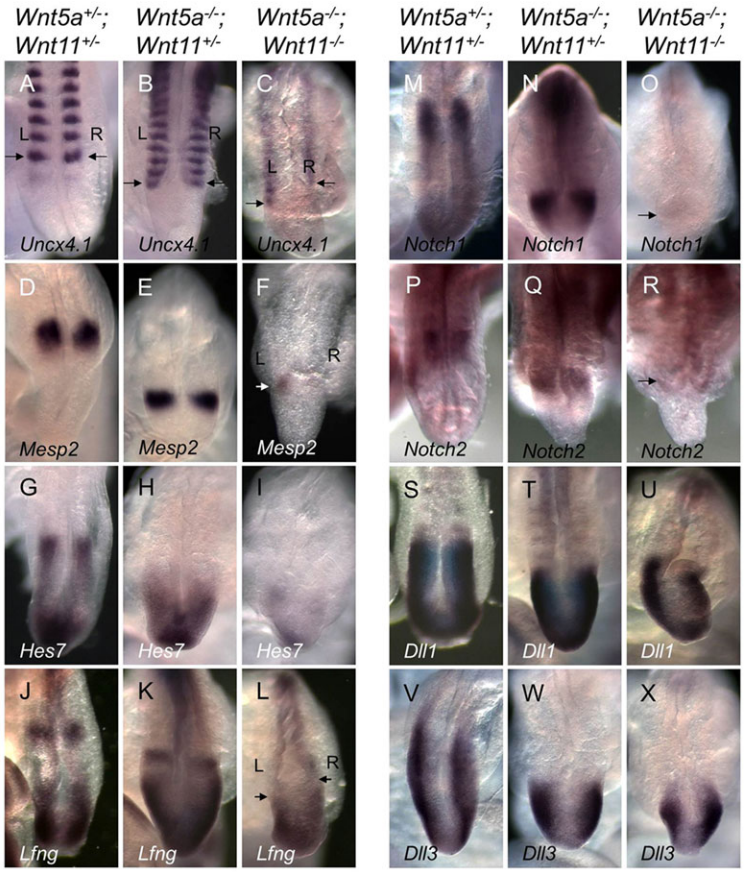

Fig. 4. Reduced and irregular somite formation in *Wnt5a*$^{-/-}$; *Wnt11*$^{-/-}$ embryos. Whole-mount *in situ* hybridization with the indicated probes in E9.5 embryos. Dorsal views of the tail bud are shown. (A-C) Expression of *Uncx4.1* is reduced in *Wnt5a*$^{-/-}$; *Wnt11*$^{-/-}$ embryos. Note the loss of symmetric somite formation in *Wnt5a*$^{-/-}$; *Wnt11*$^{-/-}$ embryos (*n*=3/6). Arrows mark caudalmost somites. (D-L) Reduced expression of *Mesp2*, *Hes7* and *Lfng* in *Wnt5a*$^{-/-}$; *Wnt11*$^{-/-}$ embryos (F,I,L). Asymmetric gene expression is indicated by arrows (F,L). (M-R) *Notch1* and *Notch2* expression is reduced in *Wnt5a*$^{-/-}$; *Wnt11*$^{-/-}$ embryos (O,R, arrows), whereas expression of *Dll1* and *Dll3* is unchanged (S-X). L, left; R, right.

Development (2015) 142, 1516-1527 doi:10.1242/dev.119065

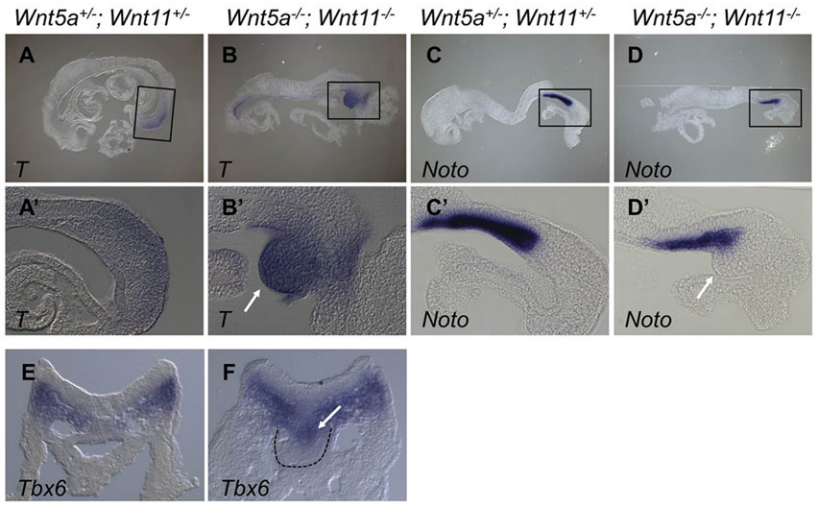

Fig. 5. Ectopic cell accumulation in *Wnt5a*$^{-/-}$; *Wnt11*$^{-/-}$ embryos. Whole-mount *in situ* hybridization showing expression of the indicated genes in E8.5 embryos. Sagittal sections show the expression of *T* (B,B′) but not of *Noto* (D,D′) in the ectopic cell accumulation in *Wnt5a*$^{-/-}$; *Wnt11*$^{-/-}$ embryos (arrows in B′,D′). (E,F) Transverse sections of the embryos shown in Fig. 3M,R. *Tbx6* expression was only found in the dorsal part of the ectopic cell accumulation (arrow in F). The ventral border of the ectopic cell accumulation is indicated by a dotted line (F). Boxes in A-D indicate the areas shown at higher magnification in A′-D′, respectively.

mass might be a result of accumulated precursors of midline and paraxial mesodermal cells failing to migrate to their proper destination. Therefore, impaired notochord and somite formation might be caused by a lack of normal motile precursor cells. To test this hypothesis, we characterized the accumulated cells in detail.

Cell labeling and genetic lineage-tracing experiments have revealed that NPCs are derived from relatively quiescent PNC cells (Sulik et al., 1994; Yamanaka et al., 2007; Ukita et al., 2009). In addition, the source of the axial and paraxial mesoderm precursors is believed to reside at the NSB (Sulik et al., 1994; Bellomo et al., 1996; Cambray and Wilson, 2007), which is where we observed the ectopic accumulation. A similar accumulation of cells has already been reported in *Wnt5*$^{-/-}$ embryos (Yamaguchi et al., 1999a). However, in the *Wnt5a*$^{-/-}$; *Wnt11*$^{-/-}$ embryos, it appeared to be more densely populated with cells and less organized. As in the *Wnt5a* mutants, the accumulated cells expressed *T*, indicating a mesodermal fate (Fig. 5A-B′) (Yamaguchi et al., 1999a). To further test whether these cells were already committed to a specific mesodermal fate, we investigated the expression of *Noto*, which is expressed exclusively in the PNC and notochord (Fig. 5C,C′) (Abdelkhalek et al., 2004). The accumulated cells did not express *Noto*, indicating that they had not differentiated into notochord cells in the *Wnt5a*$^{-/-}$; *Wnt11*$^{-/-}$ embryos (Fig. 5D,D′). Next, we investigated whether the accumulated cells had adopted a paraxial fate by analyzing the expression of *Tbx6* (Chapman and Papaioannou, 1998). *Tbx6* was expressed in the dorsal portion of the ectopically accumulated cells, suggesting that these cells were PS cells and/or early paraxial mesodermal cells, but occupying the midline position (Fig. 5E,F). Thus, in the absence of *Wnt5a* and *Wnt11* a mixed population consisting of paraxial (*T*-positive, *Tbx6*-positive) and axial (*T*-positive, *Tbx6*-negative) mesodermal cells accumulates posterior to the PNC.

Regulated by signals from the PS, mesodermal cells are generated in the PS from pluripotent epiblast stem cells that also generate ectoderm and endodermal cells (Gardner and Beddington, 1988). At later developmental stages, the differentiation potential of the descendants of these early embryonic stem cells becomes progressively restricted (Loebel et al., 2003). Bipotential axial stem cells in the caudal lateral epiblast (CLE) (Wilson et al., 2009; Takemoto et al., 2011) generate caudal neural plate and paraxial mesoderm. Therefore, we hypothesized that *Wnt5a* and *Wnt11* might regulate mesodermal cell fates by regulating the differentiation of late epiblast stem cells or CLE. To test this, we investigated the expression of Sox17 and Sox2, which are endodermal and ectodermal markers, respectively (Collignon et al., 1996; Kanai-Azuma et al., 2002). Sox17 expression was normal in the endodermal cell layer in *Wnt5a*$^{-/-}$; *Wnt11*$^{-/-}$ embryos, as compared with the control (supplementary material Fig. S9A,B). However, as mentioned above, T was downregulated in the dorsal PS in *Wnt5a*$^{-/-}$; *Wnt11*$^{-/-}$ mutants (Fig. 6A,B). By contrast, Sox2 expression was increased ventrally and posteriorly. The opposing expression gradients of T and Sox2 in the presumptive paraxial mesodermal in *Wnt5a*$^{-/-}$; *Wnt11*$^{-/-}$ embryos indicated an increase in neural ectodermal and a decrease in mesodermal cell fate determination (Fig. 6A,B). To exclude the possibility that reduced cell proliferation in the PS region caused the notochord defect, we stained embryos for PHP3. Cell proliferation appeared normal in this region in *Wnt5a*$^{-/-}$; *Wnt11*$^{-/-}$ embryos compared with the controls (supplementary material Fig. S9C,D). Therefore, we concluded that the loss of *Wnt5a* and *Wnt11* led to reduced mesoderm formation.

As mesoderm generation from the ectodermal epiblast requires EMT (Shook and Keller, 2003) and cell accumulations in the PS have been reported in mouse mutants with defective EMT during gastrulation (Arnold et al., 2008), we hypothesized that incomplete EMT might be a cellular mechanism underlying the reduced mesoderm formation in *Wnt5a*$^{-/-}$; *Wnt11*$^{-/-}$ embryos. To test this, we first examined the expression of *Snail* (also known as *Snai1*), a transcription factor that regulates the induction of EMT (Barrallo-Gimeno and Nieto, 2005). However, *Snail* expression was similar in *Wnt5a*$^{-/-}$; *Wnt11*$^{-/-}$ and control embryos (supplementary material Fig. S9E-F′), suggesting that initiation of EMT occurred normally. Next, we tested whether EMT takes place in late gastrulating embryos by examining the integrity of the basement membrane and the expression of epithelial and mesenchymal cell markers (Hay and Zuk, 1995; Smyth et al., 1999; Mendez et al., 2010). In the region posterior to the PNC in wild-type embryos at E7.75-E8.25, the basement membrane had broken down, as indicated by fragmented laminin staining (supplementary material Fig. S10A-F′). Intact basement membrane was observed anterior to the PNC (supplementary material Fig. S10A-F′). In addition, we found that basement membrane breakdown was associated with downregulation of E-cadherin expression and upregulation of vimentin expression in this region (supplementary material Fig. S10D-F′). As EMT is characterized by a downregulation of E-cadherin (Hay and Zuk, 1995) and upregulation of vimentin (Mendez et al., 2010) expression, our results indicate that

Development (2015) 142, 1516-1527 doi:10.1242/dev.119065

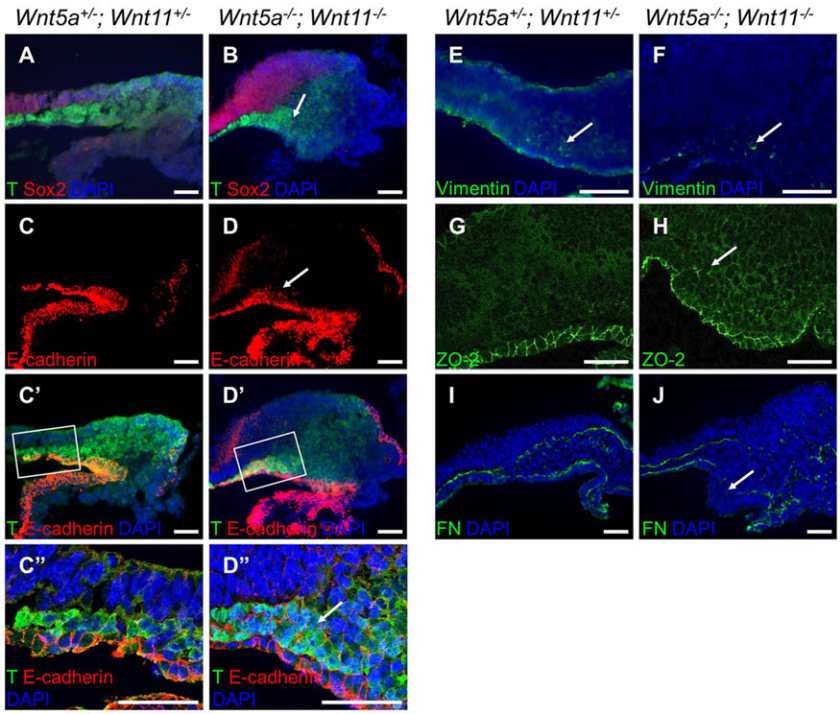

Fig. 6. Defective EMT in *Wnt5a*$^{-/-}$; *Wnt11*$^{-/-}$ embryos. Immunofluorescent staining of sagittal sections of posterior parts of E8.5 embryos. (A,B) T (green) expression is reduced in the dorsal PS region of the *Wnt5a*$^{-/-}$; *Wnt11*$^{-/-}$ embryo, whereas Sox2 (red) expression is extended ventrally and posteriorly. T expression in the ectopic cell accumulation in *Wnt5a*$^{-/-}$; *Wnt11*$^{-/-}$ embryos is marked by an arrow in B. Note that T staining was observed throughout PS cells but is overlaid by strong DAPI signals, resulting in the appearance of staining restricted to the cytosol. (C-D″) Ectopic expression of E-cadherin (red) in T (green) in *Wnt5a*$^{-/-}$; *Wnt11*$^{-/-}$ embryos (arrows in D,D″). Boxes in C′,D′ indicate areas shown at higher magnification in C″,D″, respectively. (E,F) Reduced expression of vimentin in *Wnt5a*$^{-/-}$; *Wnt11*$^{-/-}$ embryos (arrows in E,F). (G,H) Increased expression of ZO-2 in the ectopically accumulated cells in *Wnt5a*$^{-/-}$; *Wnt11*$^{-/-}$ embryos (arrow in H). (I,J) Loss of FN in the ectopic cell accumulation of *Wnt5a*$^{-/-}$; *Wnt11*$^{-/-}$ embryos (arrow in J). Scale bars: 50 µm.

active EMT occurs posterior to the PNC in wild-type embryos as a continuous process from mid to late gastrula stages, and thus NSB and anterior PS cells both undergo EMT in late gastrulation. However, in *Wnt5a*$^{-/-}$; *Wnt11*$^{-/-}$ embryos, cells within the ectopic accumulation expressed E-cadherin ectopically (Fig. 6C-D″), while vimentin expression was reduced (Fig. 6E,F). These cells also expressed T at similar levels to that in notochord cells, indicating that these cells were early progenitors of the notochord (Fig. 6D,D″, arrows). These findings indicate that EMT in this region generates notochord progenitor cells and that, in the absence of *Wnt5a* and *Wnt11*, even though EMT was induced and the cells were on their way to becoming mesoderm, they failed to fully acquire mesenchymal character. Increased cell-cell adhesion due to persistent E-cadherin expression in these cells prevents them from migration. In support of this, we found that ZO-2 (Tjp2) expression, which marks tight junctions in epithelial and endothelial cells, was increased in the ectopically accumulated cells, although normal expression was maintained in the endodermal layer in the absence of *Wnt5a* and *Wnt11* (Fig. 6G,H).

Proper cell migration not only requires downregulation of E-cadherin but also a functional extracellular matrix (ECM). After cell fate determination and germ layer formation, different germ layers are separated by ECM containing fibronectin (FN; also known as Fn1), which plays important roles in cell adhesion and migration (Pankov and Yamada, 2002). Deposition of FN has been linked to CE movements and PCP (Goto et al., 2005). In zebrafish, loss of Vangl2 and Prickle1a led to decreased FN levels (Dohn et al., 2013). In the absence of FN, mouse embryos die during gastrulation and show defects in A-P axis formation (George et al., 1993). In control embryos, a layer of FN-containing ECM separated the endodermal or ectodermal layer from the mesodermal layer (Fig. 6I). However, in *Wnt5a*$^{-/-}$; *Wnt11*$^{-/-}$ embryos the FN-containing layers were missing where mesodermal cell fate determination was incomplete (Fig. 6J). This supports the idea that reduced PCP signaling and incomplete mesodermal fate determination in the absence of *Wnt5a* and *Wnt11* leads to the reduction of FN expression. Taken together, EMT defects in the *Wnt5a*$^{-/-}$; *Wnt11*$^{-/-}$ embryos reduce axial and paraxial mesoderm formation and hamper cell migration, causing ectopic cell accumulation and a failure of axial elongation, with smaller and irregular somites.

E-cadherin downregulation during EMT requires an active p38 MAPK pathway (Zohn et al., 2006). To test whether p38 (Mapk14) is activated in the *Wnt5a*$^{-/-}$; *Wnt11*$^{-/-}$ embryos, we investigated the phosphorylation of p38 (P-p38). We observed a substantial reduction of P-p38 at the posterior end of the *Wnt5a*$^{-/-}$; *Wnt11*$^{-/-}$ embryo (Fig. 7A-B′). This indicates that *Wnt5a* and *Wnt11* are necessary to activate p38 MAPK and downregulate E-cadherin in the posterior embryo. In mouse F9 teratocarcinoma cells, Wnt5a has been shown to induce p38 phosphorylation (Ma and Wang, 2007). In order to establish whether Wnt11 also activates p38 and if Wnt5a and Wnt11 act synergistically in this process, we treated primary mouse embryonic fibroblast (MEF) cells with recombinant Wnt5a and/or Wnt11 protein (Fig. 7C,D). We found that Wnt5a can induce p38 phosphorylation and that Wnt5a and Wnt11 together induce more robust p38 phosphorylation. To further investigate this interaction, we tested whether JNK signaling, which has been identified as a target of Wnt5a and Wnt11 signaling, is involved in the activation of p38 (Pandur et al., 2002; Yamanaka et al., 2002). We observed an increase of c-Jun phosphorylation (a target of JNK) induced by Wnt5a (Fig. 7C,E). To block c-Jun activity we employed SP600125, an inhibitor of the kinase JNK (Mapk8). However, as SP600125 treatment induced phosphorylation of p38 even at very low concentrations, we were unable to test whether c-Jun activity is required for Wnt5a/Wnt11-mediated p38 phosphorylation (data not shown). Next, we investigated whether Rho GTPase activation is required for the phosphorylation of p38, as Wnt5a and Wnt11 have been shown to activate Rho GTPases (Zhu et al., 2006). Wnt11 treatment increased RhoA activation significantly, which was further enhanced by Wnt5a treatment in MEF cells (Fig. 7F,G). To test whether RhoA activity is required for p38 phosphorylation, we

Development (2015) 142, 1516-1527 doi:10.1242/dev.119065

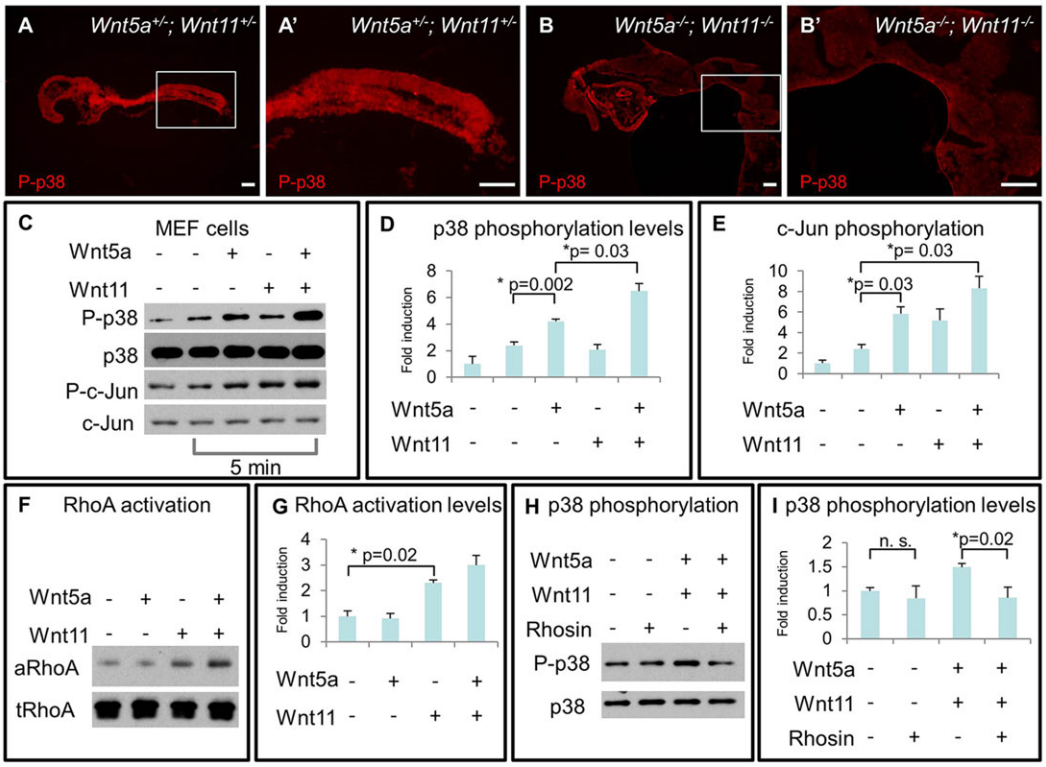

Fig. 7. Reduced p38 phosphorylation in the posterior of *Wnt5a*$^{-/-}$; *Wnt11*$^{-/-}$ embryos and induction of p38 phosphorylation by Wnt5a and Wnt11. (A-B′) Immunofluorescent staining of phosphorylated p38 (P-p38) in sagittal sections of posterior embryos at E8.5. P-p38 is reduced in the PS region of *Wnt5a*$^{-/-}$; *Wnt11*$^{-/-}$ embryos (B). Boxes in A,B indicate areas shown at higher magnification in A′,B′, respectively. (C-E) Western blot of P-p38 in MEF cells (C) showing that p38 phosphorylation and c-Jun phosphorylation are induced by recombinant Wnt5a and Wnt11 protein. Quantifications of three experiments reveal significant changes in phosphorylation levels induced by the addition of Wnt5a and Wnt11 (D,E). (F,G) Activation of RhoA is induced by Wnt11 (F). aRhoA, activated RhoA; tRhoA, total RhoA. Quantification of three experiments is shown in G. (H,I) Inhibition of RhoA activation using 1 µM Rhosin prevents Wnt5a/Wnt11-induced phosphorylation of p38 (H). Quantification of three experiments is shown in I. (D,E,G,I) Student's *t*-test; n.s., not significant. Error bars indicate s.d. Scale bars: 100 µm.

employed the RhoA inhibitor Rhosin (Shang et al., 2012). Inhibition of RhoA by Rhosin prevented Wnt5a/Wnt11-mediated p38 phosphorylation in MEF cells (Fig. 7H,I). We therefore concluded that Wnt5a and Wnt11 act synergistically to enhance p38 phosphorylation and that RhoA signaling can mediate this activity.

Finally, we examined whether Wnt5a and Wnt11 regulate EMT through PCP signaling, as both EMT and PCP pathways regulate cytoskeletal reorganization and play important roles in cell migration. We analyzed *Vangl1*$^{-/-}$; *Vangl2*$^{-/-}$ embryos and were unable to detect a similar accumulation of cells posterior to the notochord as we observed in *Wnt5a*$^{-/-}$; *Wnt11*$^{-/-}$ embryos (supplementary material Fig. S11A,B). However, there was a slight increase in E-cadherin in this region, although the increase was less profound than that in the *Wnt5a*$^{-/-}$; *Wnt11*$^{-/-}$ mutant. In addition, in the *Vangl1*$^{-/-}$; *Vangl2*$^{-/-}$ MEF cells, Wnt5a and Wnt11 could still induce p38 phosphorylation, albeit at lower levels than in wild-type MEF cells (supplementary material Fig. S11C,D; Fig. 7C). Therefore, we conclude that PCP also regulates EMT, but Wnt5a and Wnt11 regulate EMT through multiple pathways including PCP. Taken together our results indicate that, in the absence of *Wnt5a* and *Wnt11*, the cells of the prospective midline and paraxial mesoderm fail to migrate due to incomplete EMT.

DISCUSSION

Here we have found that *Wnt5a* and *Wnt11* play redundant roles in regulating multiple developmental processes in the late gastrulating embryo. Although *Wnt11*$^{-/-}$ embryos do not have obvious developmental defects, the phenotypes of the early *Wnt5a*$^{-/-}$embryos were significantly enhanced by loss of *Wnt11*. *Wnt11* is specifically expressed in the PNC (Kispert et al., 1996) and this expression accounts for its redundant role with *Wnt5a* in early embryonic development, as shown here. This explains why the defects observed are restricted to the notochord and the paraxial mesoderm that ingress in this region. *Wnt5a* and *Wnt3a* are both expressed strongly in the PS (Takada et al., 1994; Yamaguchi et al., 1999a). Wnt3a signals through the β-catenin-mediated canonical Wnt signaling pathway, whereas Wnt5a does not (Logan and Nusse, 2004; Kikuchi et al., 2012; Topol et al., 2003; Westfall et al., 2003). Therefore, even though both are required to regulate mouse gastrulation, the *Wnt5a*$^{-/-}$ and *Wnt3a*$^{-/-}$embryos exhibit distinct defects (Takada et al., 1994; Yamaguchi et al., 1999a). In *Wnt5a*$^{-/-}$; *Wnt11*$^{-/-}$embryos, *Wnt3a* is still expressed at normal levels and the canonical Wnt signaling activity is largely normal, as judged by TOPGAL activity (DasGupta and Fuchs, 1999), confirming that both *Wnt5a* and *Wnt11* act through β-catenin-independent pathways in early mouse embryos.

During the formation of the trunk notochord at E8.5, cell proliferation and cell death appeared normal in *Wnt5a*$^{-/-}$; *Wnt11*$^{-/-}$ embryos (supplementary material Fig. S7). However, at later stages we observed an increase in cell death and reduced proliferation. This reduction in cell survival might be secondary to the heart defects observed and the reduction in *Shh* expression due to earlier defects in notochord formation. In the early

Development (2015) 142, 1516-1527 doi:10.1242/dev.119065

embryos, the PCP pathway controls CE that is required for notochord formation (Ybot-Gonzalez et al., 2007). Both *wnt5a* and *wnt11* regulate CE in zebrafish (Rauch et al., 1997; Heisenberg et al., 2000), but in mammalian embryos the role of *Wnt11* in CE had not been demonstrated. We found in this study that the *Wnt11* function can be mostly fulfilled by *Wnt5a* and that *Wnt5a* and *Wnt11* both regulate CE of the trunk notochord cells and paraxial mesodermal cells through PCP (Fig. 2). However, in $Wnt5a^{-/-}$; $Wnt11^{-/-}$ embryos, asymmetrical localization of Vangl1 was still observed in some notochord cells and NT closure was normal, suggesting that other Wnt ligands present in early embryos (Yamaguchi, 2008) can also regulate PCP. Consistent with this, we did not detect any defects in neurulation, which requires PCP function. We also observed normal asymmetrical localization of Vangl1 in the ciliated PNC cells and low penetrance of left-right asymmetry defects in the $Wnt5a^{-/-}$; $Wnt11^{-/-}$ embryos.

CE defects in PCP mutants result in shortened and broadened notochord and floor plate (Greene et al., 1998; Ybot-Gonzalez et al., 2007). However, in $Wnt5a^{-/-}$; $Wnt11^{-/-}$ embryos, the notochord is shortened, but thinner, resulting in reduced *Shh* expression and hence dorsalization of the NT and somites. We found that this peculiar phenotype is caused by reduced migration and generation of NPCs from the PNC. The source of trunk and tail notochord progenitors is believed to reside in the border region between the posterior PNC and the anterior PS (Cambray and Wilson, 2007). Since the PNC (node)/streak border region is believed to contain a population of stem cells, it is also possible that both trunk and tail notochord formation are dependent on proper migration of the descendants of these stem cells, which is regulated by *Wnt5a* and *Wnt11* (Cambray and Wilson, 2007). Thus, the thinner notochord is likely to be caused by defects in two processes regulated by *Wnt5a* and *Wnt11*. First, as PCP is required to provide directionality to migrating cells, disruption of PCP due to loss of *Wnt5a* and *Wnt11* leads to reduced directed anterior and posterior migration of NPCs, such that there are fewer cells to form trunk and tail notochord. Second, as the PNC is organized as an epithelium and the migrating cells display mesenchymal properties, this process involves EMT. Indeed, in the PNC (node)/streak border region, we have observed breakdown of the basement membrane and a reduction of epithelial markers (supplementary material Fig. S10). An increase in cell adhesion molecules in the NPCs of $Wnt5a^{-/-}$; $Wnt11^{-/-}$ embryos indicates that some of the precursors of the notochord are unable to fully adopt mesenchymal cell properties, resulting in fewer cells available for trunk and tail notochord formation. A similar EMT process has recently been shown to control the generation of limb mesenchyme cells during limb bud formation (Gros and Tabin, 2014).

Wnt/β-catenin signaling is a potent inducer of EMT in early gastrulation and it suppresses E-cadherin expression. Interestingly, blocking Wnt/β-catenin signaling by removing β-catenin in *Noto*-expressing cells led to persistent strong E-cadherin expression in NPCs and reduction of notochord elongation (Ukita et al., 2009), suggesting that Wnt/β-catenin signaling also regulates EMT in the generation of NPCs at late gastrulation stages. Consistent with this, it has been reported that *Wnt3a* controls paraxial mesoderm formation and Tbx6 expression (Nowotschin et al., 2012). The data in that report reveal that cells modulate the expression of *Wnt3a* as they traverse the PS: as they enter they upregulate *Wnt3a*, and then subsequently downregulate *Wnt3a* as they exit. The study suggests that reduced tail bud formation in $Wnt3a^{-/-}$ mutants might be caused by the first steps of late paraxial mesoderm formation, such as ingression/EMT (Nowotschin et al., 2012). Compared with Wnt/β-catenin signaling, Wnt5a and Wnt11 are weak inducers of EMT. EMT occurred at early gastrulation stages in $Wnt5a^{-/-}$; $Wnt11^{-/-}$ embryos and the phenotypes were only manifested at later stages, possibly due to progressive accumulation of a weak EMT defect.

In addition to reduced migration of NPCs, we propose that reduced A-P axis elongation is also caused by reduced paraxial mesoderm formation in the absence of *Wnt5a* and *Wnt11* (Fig. 5). In the PS of the late gastrula embryo there is continuous EMT (Arnold and Robertson, 2009). Cells ingress and then delaminate from the epiblast ectoderm to form a loose mesenchyme that will later form the paraxial mesoderm. In this process, the ingressing cells turn off the *Sox2* enhancer N1, whereas *Tbx6* expression is upregulated (Takemoto et al., 2011). Once formed, the mesoderm is then separated from the neural ectoderm by a layer of FN-containing basement membrane. In $Wnt5a^{-/-}$; $Wnt11^{-/-}$ embryos, reduced T expression and expanded Sox2 expression suggest that reduced paraxial mesoderm formation might also be caused by incomplete EMT. FN deposition requires dynamic cell rearrangements and the increase in cell adhesion that we observed in this region might thus be responsible for the lack of FN (Dzamba et al., 2009). The defective EMT therefore led secondarily to incomplete formation of the FN-containing basement membrane, reduced axial mesoderm migration causing a thinner notochord, and reduced paraxial mesoderm migration causing the formation of smaller and irregular somites. Therefore, in this study we have identified that *Wnt5a* and *Wnt11* are required to control EMT in the late gastrula embryo.

Our results suggest that Wnt5a and Wnt11 regulate EMT through RhoA-mediated activation of p38. However, we cannot exclude the possibility that other pathways downstream of Wnt5a and Wnt11 might also be involved in regulating EMT, as Wnt5a and Wnt11 can stimulate multiple non-canonical Wnt pathways (reviewed by Yang, 2012). We show that JNK signaling is activated by the addition of Wnt5a and Wnt11, but it is not clear whether JNK activation is required for p38 activation. As JNK and p38 signaling pathways often act in parallel (Widenmaier et al., 2009; Das et al., 2011; Chen et al., 2013; Tanaka et al., 2013) and JNK signaling has been shown to be involved in the induction of EMT in various tissues (Pallet et al., 2012; Chen et al., 2013), both p38 and JNK might regulate EMT during embryonic A-P axis elongation.

As Wnt/β-catenin signaling is required for *T* expression and T regulates *Tbx6* expression (Yamaguchi et al., 1999b), the reduced T expression dorsally may cause ventrally extended *Sox2* expression, which is normally suppressed by Tbx6. One scenario is that *Wnt5a* and *Wnt11* can signal weakly through the canonical Wnt pathway. However, the strong *Wnt3a* expression and normal TOPGAL activity in $Wnt5a^{-/-}$; $Wnt11^{-/-}$ embryos (Fig. 3F; supplementary material Fig. S6F) suggest that *Wnt5a* and *Wnt11* might modulate *T* and *Tbx6* expression independently of the canonical Wnt pathway. Further experiments are required to clarify this point.

MATERIALS AND METHODS

Mouse lines and genotyping

Wnt5a, *Wnt11*, *Vangl1* and *Vangl2* mutant mouse strains and associated genotyping methods have been described previously (Yamaguchi et al., 1999a; Majumdar et al., 2003; Song et al., 2010). Animal care and experimental animal procedures were performed in accordance with the NHGRI institutional standards and were approved by the Institutional Animal Care and Use Committee, NHGRI, and by the NIH Institutional Review Board.

Development (2015) 142, 1516-1527 doi:10.1242/dev.119065

In situ hybridization and immunofluorescence staining

Whole-mount *in situ* hybridization was performed according to standard protocols (Topol et al., 2003).

RNA probes have been described previously: Shh (Echelard et al., 1993), T (Wilson et al., 1995), Nkx2.5 (Lyons et al., 1995), Wnt3a (Takada et al., 1994), Wnt5a (Yamaguchi et al., 1999a), Wnt11 (Kispert et al., 1996), Fgf8 (Crossley and Martin, 1995), Tbx6 (Chapman and Papaioannou, 1998), Uncx4.1 (Mansouri et al., 1997), Mesp2 (Saga et al., 1997), Hes7 (Bessho et al., 2001), Lfng (Dale et al., 2003), Noto (Abdelkhalek et al., 2004), Notch1 (Conlon et al., 1995), Notch2 (Bessho et al., 2001), Dll1 (Bettenhausen et al., 1995) and Dll3 (Dunwoodie et al., 1997). For immunofluorescence staining, embryos were fixed in 4% paraformaldehyde for 30 min at 4°C and processed for cryosectioning and immunostaining according to standard protocols (Song et al., 2010). Unless indicated otherwise, each result presented was observed in at least two individual specimens with a penetrance of 100%. Primary antibodies used: brachyury (1:150; R&D Systems, AF2085), E-cadherin (1:200; R&D Systems, AF748), fibronectin (1:500; gift from K. Yamada, Bethesda, MD, USA), Sox17 (1:50; R&D Systems, AF1924), Sox2 (1:500; Abcam, ab97959), Vangl1 [1:50 (Song et al., 2010)], ZO-2 (1:100; Cell Signaling, 2847), β-catenin (1:500; BD Biosciences, 610153), phospho-p38 (1:200; Cell Signaling, #9211), Pax6 (1:50), Pax7 (1:50), Nkx2.2 (1:100), Islet1 (1:50), Lim1/2 (1:50), Nkx6.1 (1:50) (Developmental Studies Hybridoma Bank), phospho-histone H3 (1:500; Cell Signaling, 9071) and Olig2 (1:100; Abcam, ab33427). Secondary antibodies were obtained from Life Technologies and used at 1:400.

Apoptosis was analyzed using the ApopTag Apoptosis Kit (S7111, Millipore). Images were acquired using a Zeiss LSM 510 NLO Meta system and Zeiss Imager D2.

In vitro labeling

Embryos were dissected in DMEM containing 10% FBS and 25 mM HEPES pH 7.4. DiI (Sigma) was injected at 0.2 mg/ml in 3 M sucrose using a glass micropipette into cells of the PNC. Embryos were subsequently cultured for 12 h at 37°C, 5% CO_2 in a roller culture (Rotator Genie, Scientific Industries) in 25% rat serum and 75% culture medium (DMEM with 10% FBS) (Rivera-Pérez et al., 2010). After culture, the embryos were analyzed using a Zeiss V20 stereomicroscope.

Cell culture

Mouse embryonic fibroblasts (MEFs) were grown to confluence and serum starved for 2 h. Cells were then incubated in human recombinant WNT5A (125 ng/ml; R&D Systems) and WNT11 (200 ng/ml; R&D Systems) for the indicated time period. Cells were lysed in lysis buffer (20 mM Tris-HCl pH 7.4, 150 mM NaCl, 0.5% Nonidet P-40) with Halt Protease Inhibitor Cocktail (Thermo Scientific) and Halt Phosphatase Inhibitor Cocktail (Thermo Scientific), and incubated with antibodies against p38 (1:1000; Cell Signaling, #9212), phospho-p38 (1:1000; Cell Signaling, #9211), c-Jun (1:1000; Cell Signaling, 9165) or phospho-c-Jun (1:1000; Cell Signaling, 9261).

RhoA activity was determined using a RhoA Activity Kit (New East Biosciences, 80601). RhoA activity was inhibited by incubating the cells for 2 h in 1 µM Rhosin (EMD Millipore). JNK activity was blocked using 500 nM-15 µM SP600125 (Sigma).

Acknowledgements

We thank the Y.Y. laboratory for stimulating discussions, Kenneth Yamada for providing the fibronectin antibody, and Shelley Hoogstraten-Miller and Irene Ginty for providing rat serum.

Competing interests

The authors declare no competing or financial interests.

Author contributions

P.A., H.S. and W.K. performed experiments. P.A., H.S. and Y.Y. designed experiments and analyzed data. P.A. and Y.Y. prepared the manuscript. A.K. provided reagents and edited the manuscript.

Funding

The work in the laboratory of Y.Y. (P.A., H.S., W.K. and Y.Y.) was funded by the Intramural Research Program of the National Institutes of Health. The work in the laboratory of A.K. was funded by grants from the German Research Foundation (DFG). Deposited in PMC for release after 12 months.

Supplementary material

Supplementary material available online at
http://dev.biologists.org/lookup/suppl/doi:10.1242/dev.119065/-/DC1

References

Abdelkhalek, H. B., Beckers, A., Schuster-Gossler, K., Pavlova, M. N., Burkhardt, H., Lickert, H., Rossant, J., Reinhardt, R., Schalkwyk, L. C., Müller, I. et al. (2004). The mouse homeobox gene Not is required for caudal notochord development and affected by the truncate mutation. *Genes Dev.* **18**, 1725-1736.

Arnold, S. J. and Robertson, E. J. (2009). Making a commitment: cell lineage allocation and axis patterning in the early mouse embryo. *Nat. Rev. Mol. Cell Biol.* **10**, 91-103.

Arnold, S. J., Hofmann, U. K., Bikoff, E. K. and Robertson, E. J. (2008). Pivotal roles for eomesodermin during axis formation, epithelium-to-mesenchyme transition and endoderm specification in the mouse. *Development* **135**, 501-511.

Barrallo-Gimeno, A. and Nieto, M. A. (2005). The Snail genes as inducers of cell movement and survival: implications in development and cancer. *Development* **132**, 3151-3161.

Beddington, R. S. P. and Robertson, E. J. (1999). Axis development and early asymmetry in mammals. *Cell* **96**, 195-209.

Bellomo, D., Lander, A., Harragan, I. and Brown, N. A. (1996). Cell proliferation in mammalian gastrulation: the ventral node and notochord are relatively quiescent. *Dev. Dyn.* **205**, 471-485.

Bessho, Y., Miyoshi, G., Sakata, R. and Kageyama, R. (2001). Hes7: a bHLH-type repressor gene regulated by Notch and expressed in the presomitic mesoderm. *Genes Cells* **6**, 175-185.

Bettenhausen, B., Hrabe de Angelis, M., Simon, D., Guenet, J. L. and Gossler, A. (1995). Transient and restricted expression during mouse embryogenesis of Dll1, a murine gene closely related to Drosophila Delta. *Development* **121**, 2407-2418.

Blum, M., Andre, P., Muders, K., Schweickert, A., Fischer, A., Bitzer, E., Bogusch, S., Beyer, T., van Straaten, H. W. M. and Viebahn, C. (2007). Ciliation and gene expression distinguish between node and posterior notochord in the mammalian embryo. *Differentiation* **75**, 133-146.

Borovina, A., Superina, S., Voskas, D. and Ciruna, B. (2010). Vangl2 directs the posterior tilting and asymmetric localization of motile primary cilia. *Nat. Cell Biol.* **12**, 407-412.

Cambray, N. and Wilson, V. (2002). Axial progenitors with extensive potency are localised to the mouse chordoneural hinge. *Development* **129**, 4855-4866.

Cambray, N. and Wilson, V. (2007). Two distinct sources for a population of maturing axial progenitors. *Development* **134**, 2829-2840.

Chapman, D. L. and Papaioannou, V. E. (1998). Three neural tubes in mouse embryos with mutations in the T-box gene Tbx6. *Nature* **391**, 695-697.

Chen, H.-H., Zhou, X.-L., Shi, Y.-l. and Yang, J. (2013). Roles of p38 MAPK and JNK in TGF-beta1-induced human alveolar epithelial to mesenchymal transition. *Arch. Med. Res.* **44**, 93-98.

Chiang, C., Litingtung, Y., Lee, E., Young, K. E., Corden, J. L., Westphal, H. and Beachy, P. A. (1996). Cyclopia and defective axial patterning in mice lacking Sonic hedgehog gene function. *Nature* **383**, 407-413.

Ciruna, B. and Rossant, J. (2001). FGF signaling regulates mesoderm cell fate specification and morphogenetic movement at the primitive streak. *Dev. Cell* **1**, 37-49.

Cleaver, O. and Krieg, P. A. (2001). Notochord patterning of the endoderm. *Dev. Biol.* **234**, 1-12.

Cohen, E. D., Miller, M. F., Wang, Z., Moon, R. T. and Morrisey, E. E. (2012). Wnt5a and Wnt11 are essential for second heart field progenitor development. *Development* **139**, 1931-1940.

Collignon, J., Sockanathan, S., Hacker, A., Cohen-Tannoudji, M., Norris, D., Rastan, S., Stevanovic, M., Goodfellow, P. N. and Lovell-Badge, R. (1996). A comparison of the properties of Sox-3 with Sry and two related genes, Sox-1 and Sox-2. *Development* **122**, 509-520.

Conlon, R. A., Reaume, A. G. and Rossant, J. (1995). Notch1 is required for the coordinate segmentation of somites. *Development* **121**, 1533-1545.

Crossley, P. H. and Martin, G. R. (1995). The mouse Fgf8 gene encodes a family of polypeptides and is expressed in regions that direct outgrowth and patterning in the developing embryo. *Development* **121**, 439-451.

Curtin, J. A., Quint, E., Tsipouri, V., Arkell, R. M., Cattanach, B., Copp, A. J., Henderson, D. J., Spurr, N., Stanier, P., Fisher, E. M. et al. (2003). Mutation of Celsr1 disrupts planar polarity of inner ear hair cells and causes severe neural tube defects in the mouse. *Curr. Biol.* **13**, 1129-1133.

Dale, J. K., Maroto, M., Dequeant, M.-L., Malapert, P., McGrew, M. and Pourquie, O. (2003). Periodic notch inhibition by lunatic fringe underlies the chick segmentation clock. *Nature* **421**, 275-278.

Das, J., Ghosh, J., Manna, P. and Sil, P. C. (2011). Taurine suppresses doxorubicin-triggered oxidative stress and cardiac apoptosis in rat via up-

regulation of PI3-K/Akt and inhibition of p53, p38-JNK. *Biochem. Pharmacol.* **81**, 891-909.
DasGupta, R. and Fuchs, E. (1999). Multiple roles for activated LEF/TCF transcription complexes during hair follicle development and differentiation. *Development* **126**, 4557-4568.
Dohn, M. R., Mundell, N. A., Sawyer, L. M., Dunlap, J. A. and Jessen, J. R. (2013). Planar cell polarity proteins differentially regulate extracellular matrix organization and assembly during zebrafish gastrulation. *Dev. Biol.* **383**, 39-51.
Dunwoodie, S. L., Henrique, D., Harrison, S. M. and Beddington, R. S. (1997). Mouse Dll3: a novel divergent Delta gene which may complement the function of other Delta homologues during early pattern formation in the mouse embryo. *Development* **124**, 3065-3076.
Dzamba, B. J., Jakab, K. R., Marsden, M., Schwartz, M. A. and DeSimone, D. W. (2009). Cadherin adhesion, tissue tension, and noncanonical Wnt signaling regulate fibronectin matrix organization. *Dev. Cell* **16**, 421-432.
Echelard, Y., Epstein, D. J., St-Jacques, B., Shen, L., Mohler, J., McMahon, J. A. and McMahon, A. P. (1993). Sonic hedgehog, a member of a family of putative signaling molecules, is implicated in the regulation of CNS polarity. *Cell* **75**, 1417-1430.
Ericson, J., Rashbass, P., Schedl, A., Brenner-Morton, S., Kawakami, A., van Heyningen, V., Jessell, T. M. and Briscoe, J. (1997). Pax6 controls progenitor cell identity and neuronal fate in response to graded Shh signaling. *Cell* **90**, 169-180.
Gao, B., Song, H., Bishop, K., Elliot, G., Garrett, L., English, M. A., Andre, P., Robinson, J., Sood, R., Minami, Y. et al. (2011). Wnt signaling gradients establish planar cell polarity by inducing Vangl2 phosphorylation through Ror2. *Dev. Cell* **20**, 163-176.
Gardner, R. L. and Beddington, R. S. P. (1988). Multi-lineage 'stem' cells in the mammalian embryo. *J. Cell. Sci.* **1988** Suppl. 10, 11-27.
George, E. L., Georges-Labouesse, E. N., Patel-King, R. S., Rayburn, H. and Hynes, R. O. (1993). Defects in mesoderm, neural tube and vascular development in mouse embryos lacking fibronectin. *Development* **119**, 1079-1091.
Goto, T., Davidson, L., Asashima, M. and Keller, R. (2005). Planar cell polarity genes regulate polarized extracellular matrix deposition during frog gastrulation. *Curr. Biol.* **15**, 787-793.
Greene, N. D. E., Gerrelli, D., Van Straaten, H. W. M. and Copp, A. J. (1998). Abnormalities of floor plate, notochord and somite differentiation in the loop-tail (Lp) mouse: a model of severe neural tube defects. *Mech. Dev.* **73**, 59-72.
Gros, J. and Tabin, C. J. (2014). Vertebrate limb bud formation is initiated by localized epithelial-to-mesenchymal transition. *Science* **343**, 1253-1256.
Hashimoto, M., Shinohara, K., Wang, J., Ikeuchi, S., Yoshiba, S., Meno, C., Nonaka, S., Takada, S., Hatta, K., Wynshaw-Boris, A. et al. (2010). Planar polarization of node cells determines the rotational axis of node cilia. *Nat. Cell Biol.* **12**, 170-176.
Hay, E. D. and Zuk, A. (1995). Transformations between epithelium and mesenchyme: normal, pathological, and experimentally induced. *Am. J. Kidney Dis.* **26**, 678-690.
Heisenberg, C.-P., Tada, M., Rauch, G.-J., Saúde, L., Concha, M. L., Geisler, R., Stemple, D. L., Smith, J. C. and Wilson, S. W. (2000). Silberblick/Wnt11 mediates convergent extension movements during zebrafish gastrulation. *Nature* **405**, 76-81.
Kageyama, R., Masamizu, Y. and Niwa, Y. (2007). Oscillator mechanism of Notch pathway in the segmentation clock. *Dev. Dyn.* **236**, 1403-1409.
Kanai-Azuma, M., Kanai, Y., Gad, J. M., Tajima, Y., Taya, C., Kurohmaru, M., Sanai, Y., Yonekawa, H., Yazaki, K., Tam, P. P. et al. (2002). Depletion of definitive gut endoderm in Sox17-null mutant mice. *Development* **129**, 2367-2379.
Keller, R. (2002). Shaping the vertebrate body plan by polarized embryonic cell movements. *Science* **298**, 1950-1954.
Kibar, Z., Vogan, K. J., Groulx, N., Justice, M. J., Underhill, D. A. and Gros, P. (2001). Ltap, a mammalian homolog of Drosophila Strabismus/Van Gogh, is altered in the mouse neural tube mutant Loop-tail. *Nat. Genet.* **28**, 251-255.
Kibar, Z., Torban, E., McDearmid, J. R., Reynolds, A., Berghout, J., Mathieu, M., Kirillova, I., De Marco, P., Merello, E., Hayes, J. M. et al. (2007). Mutations in VANGL1 associated with neural-tube defects. *N. Engl. J. Med.* **356**, 1432-1437.
Kikuchi, A., Yamamoto, H., Sato, A. and Matsumoto, S. (2012). Wnt5a: its signalling, functions and implication in diseases. *Acta Physiol.* **204**, 17-33.
Kispert, A., Vainio, S., Shen, L., Rowitch, D. H. and McMahon, A. P. (1996). Proteoglycans are required for maintenance of Wnt-11 expression in the ureter tips. *Development* **122**, 3627-3637.
Klein, T. J. and Mlodzik, M. (2005). Planar cell polarization: an emerging model points in the right direction. *Annu. Rev. Cell Dev. Biol.* **21**, 155-176.
Lawson, K. A., Meneses, J. J. and Pedersen, R. A. (1991). Clonal analysis of epiblast fate during germ layer formation in the mouse embryo. *Development* **113**, 891-911.
Lei, Y.-P., Zhang, T., Li, H., Wu, B.-L., Jin, L. and Wang, H.-Y. (2010). VANGL2 mutations in human cranial neural-tube defects. *N. Engl. J. Med.* **362**, 2232-2235.
Loebel, D. A. F., Watson, C. M., De Young, R. A. and Tam, P. P. L. (2003). Lineage choice and differentiation in mouse embryos and embryonic stem cells. *Dev. Biol.* **264**, 1-14.
Logan, C. Y. and Nusse, R. (2004). The Wnt signaling pathway in development and disease. *Annu. Rev. Cell Dev. Biol.* **20**, 781-810.
Logan, M., Pagán-Westphal, S. M., Smith, D. M., Paganessi, L. and Tabin, C. J. (1998). The transcription factor Pitx2 mediates situs-specific morphogenesis in response to left-right asymmetric signals. *Cell* **94**, 307-317.
Lowe, L. A., Supp, D. M., Sampath, K., Yokoyama, T., Wright, C. V. E., Potter, S. S., Overbeek, P. and Kuehn, M. R. (1996). Conserved left-right asymmetry of nodal expression and alterations in murine situs inversus. *Nature* **381**, 158-161.
Lyons, I., Parsons, L. M., Hartley, L., Li, R., Andrews, J. E., Robb, L. and Harvey, R. P. (1995). Myogenic and morphogenetic defects in the heart tubes of murine embryos lacking the homeo box gene Nkx2-5. *Genes Dev.* **9**, 1654-1666.
Ma, L. and Wang, H.-Y. (2007). Mitogen-activated protein kinase p38 regulates the Wnt/cyclic GMP/Ca2+ non-canonical pathway. *J. Biol. Chem.* **282**, 28980-28990.
Mahaffey, J. P., Grego-Bessa, J., Liem, K. F., Jr and Anderson, K. V. (2013). Cofilin and Vangl2 cooperate in the initiation of planar cell polarity in the mouse embryo. *Development* **140**, 1262-1271.
Majumdar, A., Vainio, S., Kispert, A., McMahon, J. and McMahon, A. P. (2003). Wnt11 and Ret/Gdnf pathways cooperate in regulating ureteric branching during metanephric kidney development. *Development* **130**, 3175-3185.
Mansouri, A., Yokota, Y., Wehr, R., Copeland, N. G., Jenkins, N. A. and Gruss, P. (1997). Paired-related murine homeobox gene expressed in the developing sclerotome, kidney, and nervous system. *Dev. Dyn.* **210**, 53-65.
McNeill, H. (2010). Planar cell polarity: keeping hairs straight is not so simple. *Cold Spring Harb. Perspect. Biol.* **2**, a003376.
Mendez, M. G., Kojima, S. and Goldman, R. D. (2010). Vimentin induces changes in cell shape, motility, and adhesion during the epithelial to mesenchymal transition. *FASEB J.* **24**, 1838-1851.
Minowada, G., Jarvis, L. A., Chi, C. L., Neubuser, A., Sun, X., Hacohen, N., Krasnow, M. A. and Martin, G. R. (1999). Vertebrate Sprouty genes are induced by FGF signaling and can cause chondrodysplasia when overexpressed. *Development* **126**, 4465-4475.
Montcouquiol, M., Rachel, R. A., Lanford, P. J., Copeland, N. G., Jenkins, N. A. and Kelley, M. W. (2003). Identification of Vangl2 and Scrb1 as planar polarity genes in mammals. *Nature* **423**, 173-177.
Nonaka, S., Shiratori, H., Saijoh, Y. and Hamada, H. (2002). Determination of left-right patterning of the mouse embryo by artificial nodal flow. *Nature* **418**, 96-99.
Nonaka, S., Yoshiba, S., Watanabe, D., Ikeuchi, S., Goto, T., Marshall, W. F. and Hamada, H. (2005). De novo formation of left-right asymmetry by posterior tilt of nodal cilia. *PLoS Biol.* **3**, e268.
Nowotschin, S., Ferrer-Vaquer, A., Concepcion, D., Papaioannou, V. E. and Hadjantonakis, A.-K. (2012). Interaction of Wnt3a, Msgn1 and Tbx6 in neural versus paraxial mesoderm lineage commitment and paraxial mesoderm differentiation in the mouse embryo. *Dev. Biol.* **367**, 1-14.
Pallet, N., Thervet, E. and Anglicheau, D. (2012). c-Jun-N-terminal kinase signaling is involved in cyclosporine-induced epithelial phenotypic changes. *J. Transplant.* **2012**, 348604.
Pandur, P., Läsche, M., Eisenberg, L. M. and Kühl, M. (2002). Wnt-11 activation of a non-canonical Wnt signalling pathway is required for cardiogenesis. *Nature* **418**, 636-641.
Pankov, R. and Yamada, K. M. (2002). Fibronectin at a glance. *J. Cell Sci.* **115**, 3861-3863.
Placzek, M., Jessell, T. M. and Dodd, J. (1993). Induction of floor plate differentiation by contact-dependent, homeogenetic signals. *Development* **117**, 205-218.
Plouhinec, J.-L., Granier, C., Le Mentec, C., Lawson, K. A., Sabéran-Djoneidi, D., Aghion, J., Shi, D. L., Collignon, J. and Mazan, S. (2004). Identification of the mammalian Not gene via a phylogenomic approach. *Gene Expr. Patterns* **5**, 11-22.
Qian, D., Jones, C., Rzadzinska, A., Mark, S., Zhang, X., Steel, K. P., Dai, X. and Chen, P. (2007). Wnt5a functions in planar cell polarity regulation in mice. *Dev. Biol.* **306**, 121-133.
Rauch, G. J., Hammerschmidt, M., Blader, P., Schauerte, H. E., Strahle, U., Ingham, P. W., McMahon, A. P. and Haffter, P. (1997). Wnt5 is required for tail formation in the zebrafish embryo. *Cold Spring Harb. Symp. Quant. Biol.* **62**, 227-234.
Rivera-Pérez, J. A., Jones, V. and Tam, P. P. L. (2010). Culture of whole mouse embryos at early postimplantation to organogenesis stages: developmental staging and methods. *Methods Enzymol.* **476**, 185-203.
Roszko, I., Sawada, A. and Solnica-Krezel, L. (2009). Regulation of convergence and extension movements during vertebrate gastrulation by the Wnt/PCP pathway. *Semin. Cell Dev. Biol.* **20**, 986-997.
Saga, Y., Hata, N., Koseki, H. and Taketo, M. M. (1997). Mesp2: a novel mouse gene expressed in the presegmented mesoderm and essential for segmentation initiation. *Genes Dev.* **11**, 1827-1839.
Sausedo, R. A. and Schoenwolf, G. C. (1994). Quantitative analyses of cell behaviors underlying notochord formation and extension in mouse embryos. *Anat. Rec.* **239**, 103-112.

Seifert, J. R. K. and Mlodzik, M. (2007). Frizzled/PCP signalling: a conserved mechanism regulating cell polarity and directed motility. *Nat. Rev. Genet.* **8**, 126-138.
Shang, X., Marchioni, F., Sipes, N., Evelyn, C. R., Jerabek-Willemsen, M., Duhr, S., Seibel, W., Wortman, M. and Zheng, Y. (2012). Rational design of small molecule inhibitors targeting RhoA subfamily Rho GTPases. *Chem. Biol.* **19**, 699-710.
Shook, D. and Keller, R. (2003). Mechanisms, mechanics and function of epithelial-mesenchymal transitions in early development. *Mech. Dev.* **120**, 1351-1383.
Sirbu, I. O. and Duester, G. (2006). Retinoic-acid signalling in node ectoderm and posterior neural plate directs left-right patterning of somitic mesoderm. *Nat. Cell Biol.* **8**, 271-277.
Smyth, N., Vatansever, H. S., Murray, P., Meyer, M., Frie, C., Paulsson, M. and Edgar, D. (1999). Absence of basement membranes after targeting the LAMC1 gene results in embryonic lethality due to failure of endoderm differentiation. *J. Cell Biol.* **144**, 151-160.
Song, H., Hu, J., Chen, W., Elliott, G., Andre, P., Gao, B. and Yang, Y. (2010). Planar cell polarity breaks bilateral symmetry by controlling ciliary positioning. *Nature* **466**, 378-382.
Sulik, K., Dehart, D. B., Iangaki, T., Carson, J. L., Vrablic, T., Gesteland, K. and Schoenwolf, G. C. (1994). Morphogenesis of the murine node and notochord plate. *Dev. Dyn.* **201**, 260-278.
Sun, X., Meyers, E. N., Lewandoski, M. and Martin, G. R. (1999). Targeted disruption of Fgf8 causes failure of cell migration in the gastrulating mouse embryo. *Genes Dev.* **13**, 1834-1846.
Tada, M. and Smith, J. C. (2000). Xwnt11 is a target of Xenopus Brachyury: regulation of gastrulation movements via Dishevelled, but not through the canonical Wnt pathway. *Development* **127**, 2227-2238.
Takada, S., Stark, K. L., Shea, M. J., Vassileva, G., McMahon, J. A. and McMahon, A. P. (1994). Wnt-3a regulates somite and tailbud formation in the mouse embryo. *Genes Dev.* **8**, 174-189.
Takemoto, T., Uchikawa, M., Yoshida, M., Bell, D. M., Lovell-Badge, R., Papaioannou, V. E. and Kondoh, H. (2011). Tbx6-dependent Sox2 regulation determines neural or mesodermal fate in axial stem cells. *Nature* **470**, 394-398.
Tam, P. P. and Beddington, R. S. (1987). The formation of mesodermal tissues in the mouse embryo during gastrulation and early organogenesis. *Development* **99**, 109-126.
Tam, P. P. L. and Behringer, R. R. (1997). Mouse gastrulation: the formation of a mammalian body plan. *Mech. Dev.* **68**, 3-25.
Tam, P. P. L. and Loebel, D. A. F. (2007). Gene function in mouse embryogenesis: get set for gastrulation. *Nat. Rev. Genet.* **8**, 368-381.
Tam, P. P., Goldman, D., Camus, A. and Schoenwolf, G. C. (2000). Early events of somitogenesis in higher vertebrates: allocation of precursor cells during gastrulation and the organization of a meristic pattern in the paraxial mesoderm. *Curr. Top. Dev. Biol.* **47**, 1-32.
Tanaka, H., Iwasaki, Y., Yamato, H., Mori, Y., Komaba, H., Watanabe, H., Maruyama, T. and Fukagawa, M. (2013). p-Cresyl sulfate induces osteoblast dysfunction through activating JNK and p38 MAPK pathways. *Bone* **56**, 347-354.
Thiery, J. P., Acloque, H., Huang, R. Y. J. and Nieto, M. A. (2009). Epithelial-mesenchymal transitions in development and disease. *Cell* **139**, 871-890.
Topol, L., Jiang, X., Choi, H., Garrett-Beal, L., Carolan, P. J. and Yang, Y. (2003). Wnt-5a inhibits the canonical Wnt pathway by promoting GSK-3-independent beta-catenin degradation. *J. Cell Biol.* **162**, 899-908.
Tree, D. R. P., Ma, D. and Axelrod, J. D. (2002). A three-tiered mechanism for regulation of planar cell polarity. *Semin. Cell Dev. Biol.* **13**, 217-224.
Ukita, K., Hirahara, S., Oshima, N., Imuta, Y., Yoshimoto, A., Jang, C.-W., Oginuma, M., Saga, Y., Behringer, R. R., Kondoh, H. et al. (2009). Wnt signaling maintains the notochord fate for progenitor cells and supports the posterior extension of the notochord. *Mech. Dev.* **126**, 791-803.
Vermot, J. and Pourquié, O. (2005). Retinoic acid coordinates somitogenesis and left-right patterning in vertebrate embryos. *Nature* **435**, 215-220.
Vermot, J., Gallego Llamas, J., Fraulob, V., Niederreither, K., Chambon, P. and Dollé, P. (2005). Retinoic acid controls the bilateral symmetry of somite formation in the mouse embryo. *Science* **308**, 563-566.
Walentek, P., Schneider, I., Schweickert, A. and Blum, M. (2013). Wnt11b is involved in cilia-mediated symmetry breakage during Xenopus left-right development. *PLoS ONE* **8**, e73646.
Wallingford, J. B., Fraser, S. E. and Harland, R. M. (2002). Convergent extension: the molecular control of polarized cell movement during embryonic development. *Dev. Cell* **2**, 695-706.
Wang, J., Hamblet, N. S., Mark, S., Dickinson, M. E., Brinkman, B. C., Segil, N., Fraser, S. E., Chen, P., Wallingford, J. B. and Wynshaw-Boris, A. (2006). Dishevelled genes mediate a conserved mammalian PCP pathway to regulate convergent extension during neurulation. *Development* **133**, 1767-1778.
Westfall, T. A., Brimeyer, R., Twedt, J., Gladon, J., Olberding, A., Furutani-Seiki, M. and Slusarski, D. C. (2003). Wnt-5/pipetail functions in vertebrate axis formation as a negative regulator of Wnt/beta-catenin activity. *J. Cell Biol.* **162**, 889-898.
White, J. A., Ramshaw, H., Taimi, M., Stangle, W., Zhang, A., Everingham, S., Creighton, S., Tam, S.-P., Jones, G. and Petkovich, M. (2000). Identification of the human cytochrome P450, P450RAI-2, which is predominantly expressed in the adult cerebellum and is responsible for all-trans-retinoic acid metabolism. *Proc. Natl. Acad. Sci. USA* **97**, 6403-6408.
Widenmaier, S. B., Ao, Z., Kim, S.-J., Warnock, G. and McIntosh, C. H. (2009). Suppression of p38 MAPK and JNK via Akt-mediated inhibition of apoptosis signal-regulating kinase 1 constitutes a core component of the beta-cell pro-survival effects of glucose-dependent insulinotropic polypeptide. *J. Biol. Chem.* **284**, 30372-30382.
Wilson, V., Manson, L., Skarnes, W. C. and Beddington, R. S. (1995). The T gene is necessary for normal mesodermal morphogenetic cell movements during gastrulation. *Development* **121**, 877-886.
Wilson, V., Olivera-Martinez, I. and Storey, K. G. (2009). Stem cells, signals and vertebrate body axis extension. *Development* **136**, 1591-1604.
Yamaguchi, T. P. (2008). Genetics of Wnt signaling during early mammalian development. *Methods Mol. Biol.* **468**, 287-305.
Yamaguchi, T. P., Bradley, A., McMahon, A. P. and Jones, S. (1999a). A Wnt5a pathway underlies outgrowth of multiple structures in the vertebrate embryo. *Development* **126**, 1211-1223.
Yamaguchi, T. P., Takada, S., Yoshikawa, Y., Wu, N. and McMahon, A. P. (1999b). T (Brachyury) is a direct target of Wnt3a during paraxial mesoderm specification. *Genes Dev.* **13**, 3185-3190.
Yamanaka, H., Moriguchi, T., Masuyama, N., Kusakabe, M., Hanafusa, H., Takada, R., Takada, S. and Nishida, E. (2002). JNK functions in the non-canonical Wnt pathway to regulate convergent extension movements in vertebrates. *EMBO Rep.* **3**, 69-75.
Yamanaka, Y., Tamplin, O. J., Beckers, A., Gossler, A. and Rossant, J. (2007). Live imaging and genetic analysis of mouse notochord formation reveals regional morphogenetic mechanisms. *Dev. Cell* **13**, 884-896.
Yang, Y. (2012). Wnt signaling in development and disease. *Cell. Biosci.* **2**, 14.
Ybot-Gonzalez, P., Savery, D., Gerrelli, D., Signore, M., Mitchell, C. E., Faux, C. H., Greene, N. D. E. and Copp, A. J. (2007). Convergent extension, planar-cell-polarity signalling and initiation of mouse neural tube closure. *Development* **134**, 789-799.
Zhao, D., McCaffery, P., Ivins, K. J., Neve, R. L., Hogan, P., Chin, W. W. and Dräger, U. C. (1996). Molecular identification of a major retinoic-acid-synthesizing enzyme, a retinaldehyde-specific dehydrogenase. *Eur. J. Biochem.* **240**, 15-22.
Zhu, S., Liu, L., Korzh, V., Gong, Z. and Low, B. C. (2006). RhoA acts downstream of Wnt5 and Wnt11 to regulate convergence and extension movements by involving effectors Rho kinase and Diaphanous: use of zebrafish as an in vivo model for GTPase signaling. *Cell Signal.* **18**, 359-372.
Zohn, I. E., Li, Y., Skolnik, E. Y., Anderson, K. V., Han, J. and Niswander, L. (2006). p38 and a p38-interacting protein are critical for downregulation of E-cadherin during mouse gastrulation. *Cell* **125**, 957-969.

Fig. S1. Expression of *Wnt5a* and *Wnt11*. Whole mount *in situ* hybridization showing expression of *Wnt5a* **(A-D)** and *Wnt11* **(E-F)** at indicated stages. *Wnt5a* is expressed at the posterior part of the embryo and forms a gradient towards the anterior (A-D). Expression of *Wnt11* is observed in the posterior region, allantois and the PNC (E-H). LS, Late Streak; LB, Late Bud; EHF, Early Headfold; LHF, Late Headfold.

Fig. S2. Reduced length/width ratio in the *Wnt5a*$^{-/-}$*; Wnt11*$^{-/-}$ embryos. Length **(A, B, C)** and width **(A', B', C')** measurements shown by red line in embryos of indicated genotypes at the 6-Somite stage. **(D)** Reduced length/width ratio in the *Wnt5a*$^{-/-}$*; Wnt11*$^{-/-}$ embryos (n=4; student's t test p=0.04).

Fig. S3. DiI labeling in of notochord cells. (A-D) sections of embryos labeled with DiI and cultured for 12h combined with immunofluorescent staining of T positive cells. (A, B) Sagittal sections of embryos shown in Fig. 2C, D with DiI and T co-staining (arrows). Transversal sections of DiI labeled embryos show co-localization of T and DiI (arrows).

Fig. S4. Normal left-right asymmetry in most of the *Wnt5a*$^{-/-}$*; Wnt11*$^{-/-}$ embryos. (A-C) Whole-mount *in situ* hybridization showing left sided expression of *Nodal* in ventral views of E8.5 control and *Wnt5a*$^{-/-}$*; Wnt11*$^{-/-}$ embryos. Inversed expression of *Nodal* in one *Wnt5a*$^{-/-}$*; Wnt11*$^{-/-}$ embryo (C, n=1/4). **(D, E)** Immunofluorescent staining of Vangl1 in the PNC reveals

normal asymmetric localization of Vangl1 (arrows in D, E) in control and *Wnt5a*$^{-/-}$*; Wnt11*$^{-/-}$ embryos at E8.0. a, anterior; p, posterior.

Fig. S5. Dorsalized neural tube in the *Wnt5a*$^{-/-}$*; Wnt11*$^{-/-}$ embryos. **(A-L)** Immunofluorescent staining of dorsal (Pax6; A-C) and ventral markers (Nkx2.2, Olig2, Nkx6.1; D-L) of the neural tube at E9.5 showing increased expression of the dorsal marker at the expense of ventral markers in *Wnt5a*$^{-/-}$*; Wnt11*$^{-/-}$ embryos (C, F, I, L). (M) Quantifications of ratio between labeled and unlabeled cells in the NT show reduction of ventral fated cells in *Wnt5a*$^{-/-}$*; Wnt11*$^{-/-}$ embryos.

Fig. S6. Normal Fgf and canonical Wnt signaling in the *Wnt5a*$^{-/-}$*; Wnt11*$^{-/-}$ embryos. Whole-mount *in situ* hybridization of *Spr4* **(A-C)** and X-Gal staining of β-galactosidase activity in TOPGAL mice **(D-F)** in lateral views of the tail bud at E9.5. Normal expression of *Spr4* in the *Wnt5a*$^{-/-}$*; Wnt11*$^{-/-}$ embryo (C). Normal activity level of β-galactosidase in the *Wnt5a*$^{-/-}$*; Wnt11*$^{-/-}$ embryo (F).

Fig. S7. Increased apoptosis and reduced proliferation in the posterior *Wnt5a*$^{-/-}$*; Wnt11*$^{-/-}$ embryos. **(A-R)** Immunofluorescent staining of Phospho-Histone H3 (PPH3, cell proliferation, D-F, J-L, P-R) and TUNEL staining (apoptosis A-C, G-I, M-O) at E8.5 (A-F), E9.5 (G-L) and E10.5 (M-R) showing increased cell death and reduced proliferation in *Wnt5a*$^{-/-}$*; Wnt11*$^{-/-}$ embryos (C, F, I, L, O, R). Transversal sections of posterior embryos in (A-F), sagittal sections of tail bud in (G-R).

Fig. S8. Reduced retinoic acid signaling in the *Wnt5a*$^{-/-}$*; Wnt11*$^{-/-}$ embryos. Whole mount *in situ* hybridization of *Raldh2* **(A-C)**, *Cyp26* and *Uncx4*.1 **(D-F)** in dorsal views of the tail bud at E9.5 showing reduced expression of *Raldh2* in the *Wnt5a*$^{-/-}$*; Wnt11*$^{-/-}$ embryos (C) and normal expression of *Cyp26* in the *Wnt5a*$^{-/-}$*; Wnt11*$^{-/-}$ embryos (F). Arrows in (D-F) point at *Cyp26* expression.

Fig. S9. Normal expression of Sox17 and *Snail* in the *Wnt5a*$^{-/-}$*; Wnt11*$^{-/-}$ embryo. (A-D) Immunofluorescent staining of Sox17 and Phospho-Histone H3 (PPH3) in sagittal sections of posterior E8.5 embryos (A, D) shows normal endodermal fate determination and proliferation in the *Wnt5a*$^{-/-}$*; Wnt11*$^{-/-}$ embryo (B, D). **(E-F')** Whole mount *in situ* hybridization of *Snail* at E8.5 in lateral (E, F) and ventral (E', F') views showing normal expression in the *Wnt5a*$^{-/-}$*; Wnt11*$^{-/-}$ embryo (F, F').

Fig. S10. EMT occurring posterior to the PNC in WT embryos. **(A-F')** Immunofluorescent staining of Laminin, Vimentin and E-cadherin in WT embryos of different stages (E7.5 – E8.25) indicates a lack of basal membrane posterior to the PNC (marked by asterisks). Note the presence of a basal membrane in the PNC and anteriorly (arrowheads), which is absent posterior to the PNC (arrows). Scale bars in (A-F') represent 50 μm. Boxes in (A-F) indicate areas shown at higher magnification in (A'-F'), respectively.LS, Late Streak; EB, Early Bud; EHF, Early Headfold; 1S, 1-Somite; 2S, 2-Somite; 3S, 3-Somite.

Fig. S11. Lack of ectopic accumulations in posterior in *Vangl1*$^{-/-}$*; Vangl2*$^{-/-}$ embryos . (A, B) Immunofluorescent staining of sagittal sections of posterior parts of E8.5 embryos. No ectopic

cell accumulations in *Vangl1*$^{-/-}$*; Vangl2*$^{-/-}$ embryos but slight increase of E-cadherin in the posterior region (arrow in B and B'). Boxed regions in (A, B) are shown with higher magnification in (A', B') respectively. **(C, D)** Induction of p38 phosphorylation in *Vangl1*$^{-/-}$*; Vangl2*$^{-/-}$ MEF cells. Quantification of three experiments shown in (D).

Fig. S1

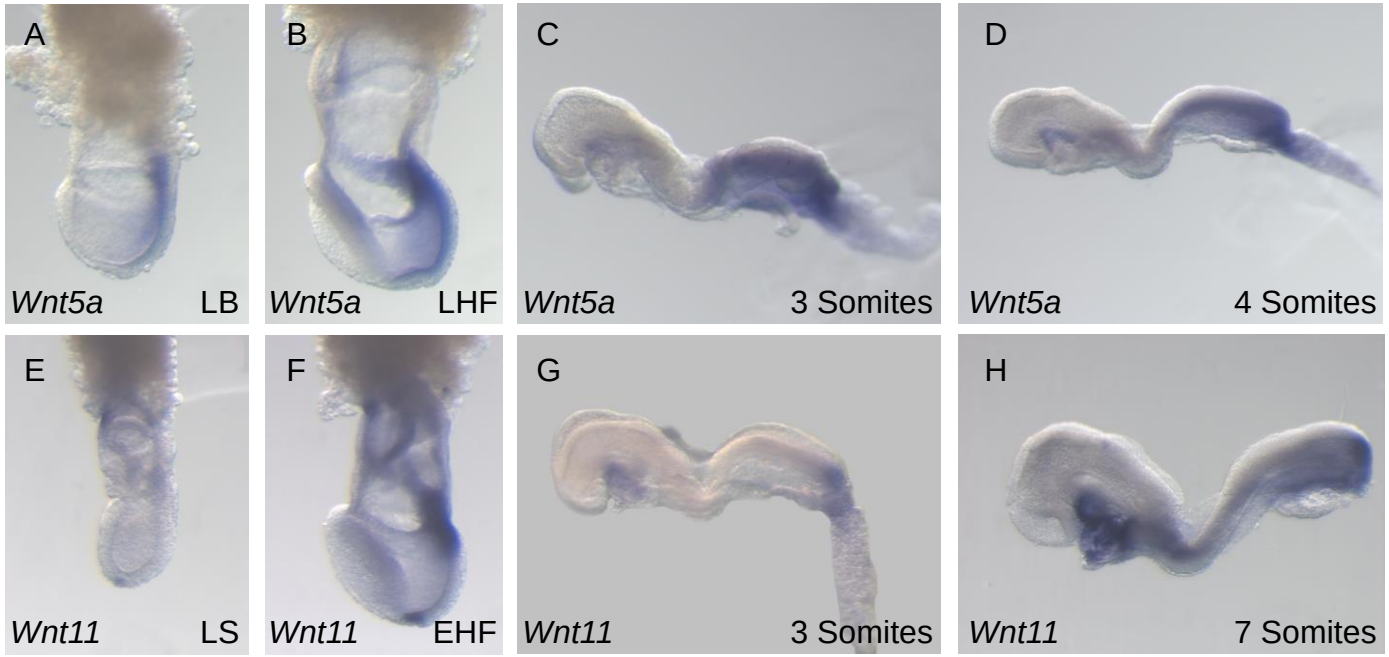
A
Wnt5a LB
B
Wnt5a LHF
C
Wnt5a 3 Somites
D
Wnt5a 4 Somites
E
Wnt11 LS
F
Wnt11 EHF
G
Wnt11 3 Somites
H
Wnt11 7 Somites

Fig. S2

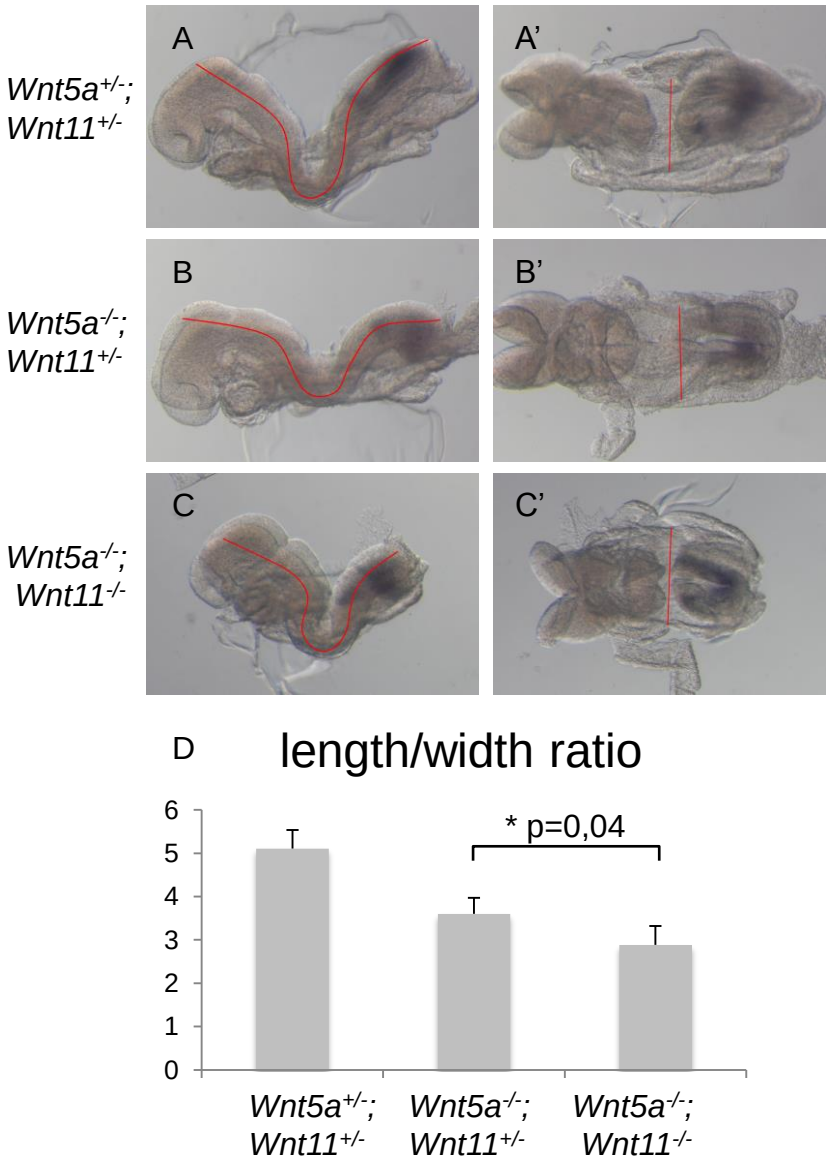
A
A'
Wnt5a+/-;
Wnt11+/-
B
B'
Wnt5a-/-;
Wnt11+/-
C
C'
Wnt5a-/-;
Wnt11-/-
D
length/width ratio
* p=0,04
6
5
4
3
2
1
0
Wnt5a+/-;
Wnt11+/-
Wnt5a-/-;
Wnt11+/-
Wnt5a-/-;
Wnt11-/-

Fig. S3

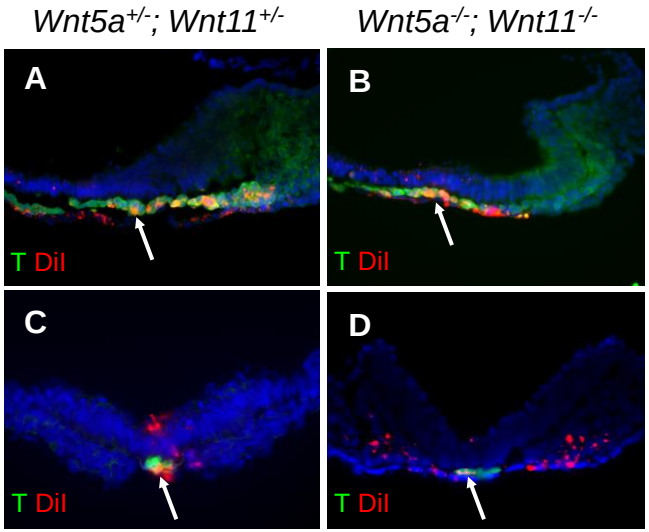

Fig. S4

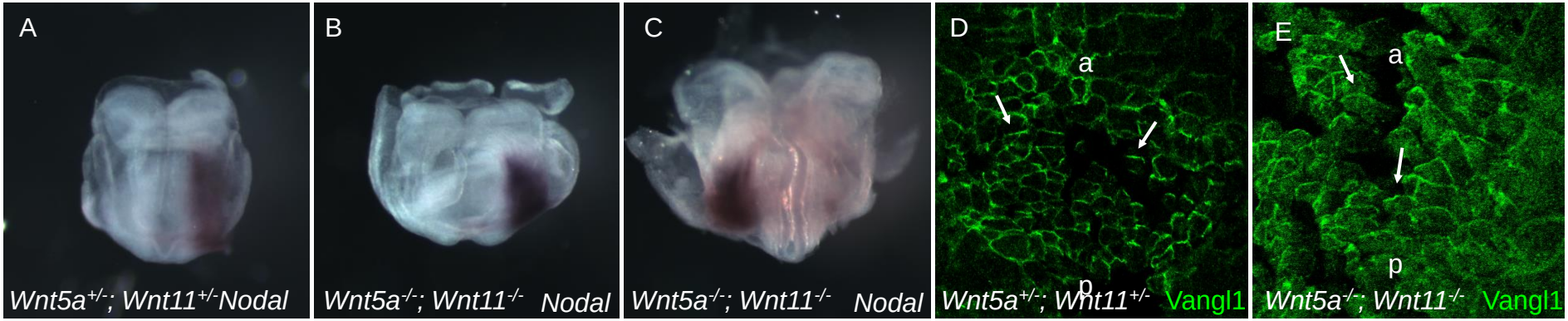
A
B
C
D
E
a
p
Wnt5a+/-; Wnt11+/- Nodal
Wnt5a-/-; Wnt11-/- Nodal
Wnt5a-/-; Wnt11-/- Nodal
Wnt5a+/-; Wnt11+/- Vangl1
Wnt5a-/-; Wnt11-/- Vangl1

Fig. S5

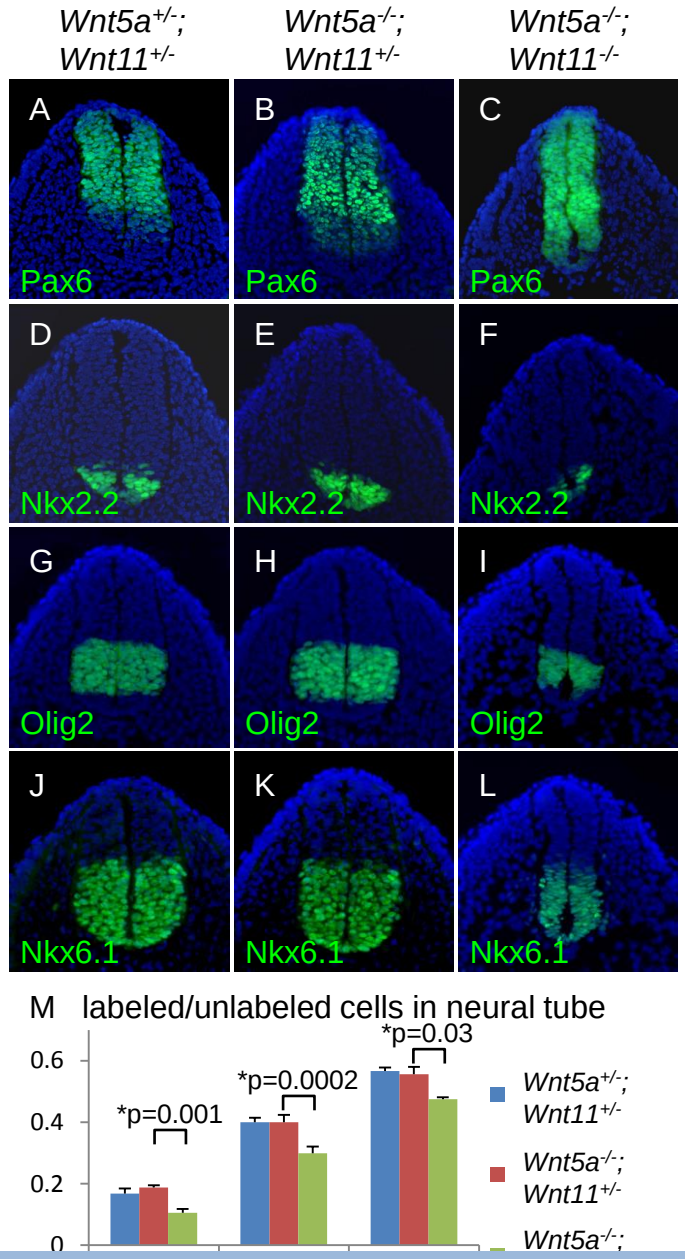
Wnt5a+/-; Wnt11+/-
Wnt5a-/-; Wnt11+/-
Wnt5a-/-; Wnt11-/-
A
Pax6
B
Pax6
C
Pax6
D
Nkx2.2
E
Nkx2.2
F
Nkx2.2
G
Olig2
H
Olig2
I
Olig2
J
Nkx6.1
K
Nkx6.1
L
Nkx6.1
M labeled/unlabeled cells in neural tube
0.6
0.4
0.2
0
*p=0.001
*p=0.0002
*p=0.03
Wnt5a+/-; Wnt11+/-
Wnt5a-/-; Wnt11+/-
Wnt5a-/-;

Fig. S6

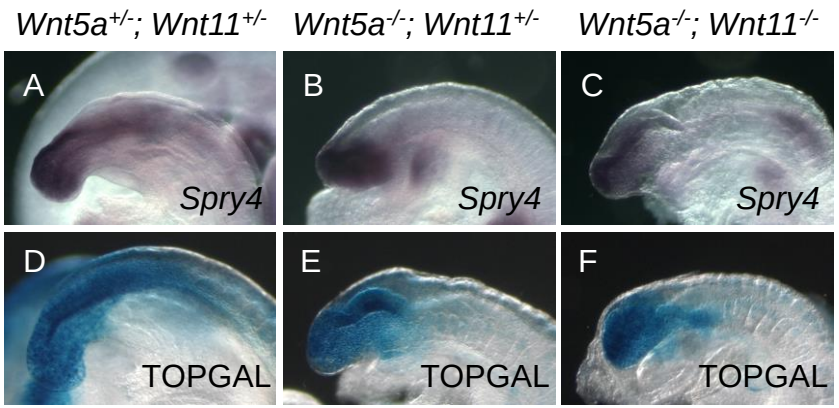
Wnt5a$^{+/-}$; *Wnt11*$^{+/-}$
Wnt5a$^{-/-}$; *Wnt11*$^{+/-}$
Wnt5a$^{-/-}$; *Wnt11*$^{-/-}$
A
Spry4
B
Spry4
C
Spry4
D
TOPGAL
E
TOPGAL
F
TOPGAL

Fig. S7

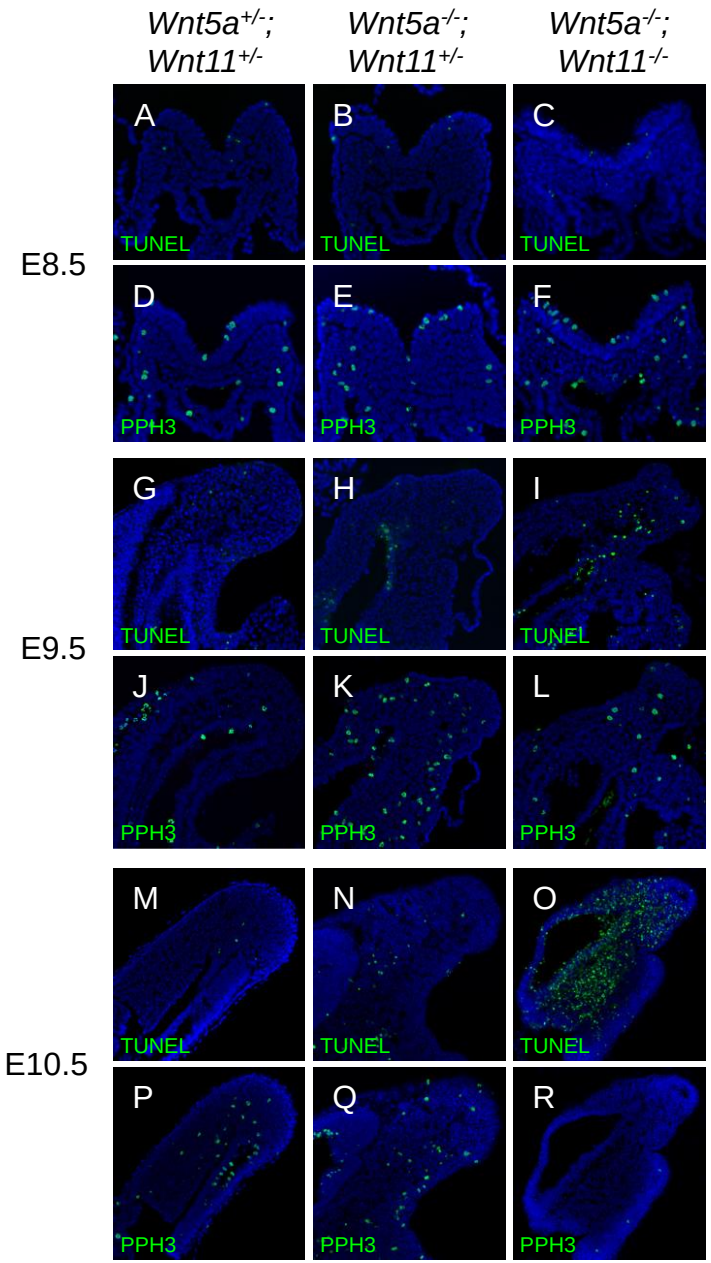
Wnt5a+/-; Wnt11+/-
Wnt5a-/-; Wnt11+/-
Wnt5a-/-; Wnt11-/-
E8.5
E9.5
E10.5
A
B
C
D
E
F
G
H
I
J
K
L
M
N
O
P
Q
R
TUNEL
PPH3

Fig. S8

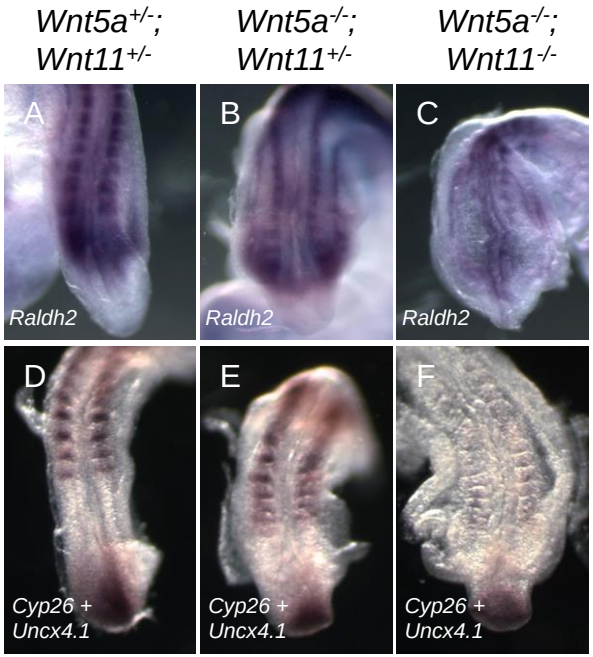
Wnt5a$^{+/-}$; *Wnt11*$^{+/-}$
Wnt5a$^{-/-}$; *Wnt11*$^{+/-}$
Wnt5a$^{-/-}$; *Wnt11*$^{-/-}$
A
Raldh2
B
Raldh2
C
Raldh2
D
Cyp26 + Uncx4.1
E
Cyp26 + Uncx4.1
F
Cyp26 + Uncx4.1

Fig. S9

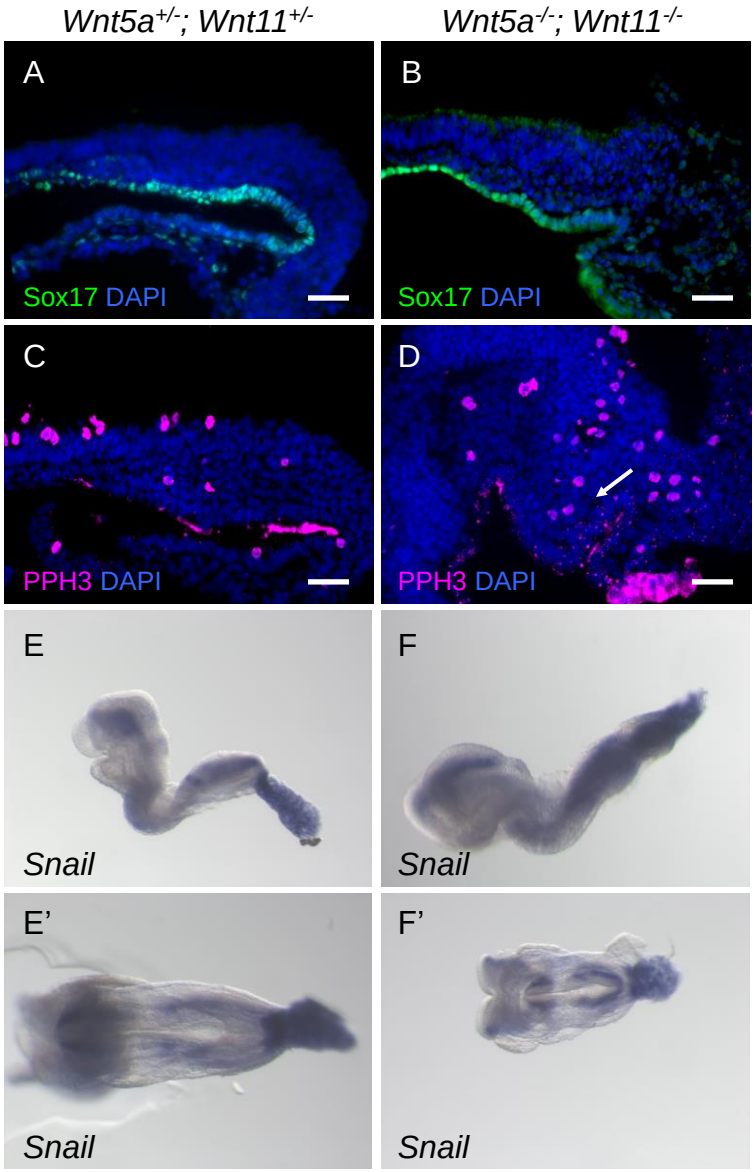
Wnt5a+/-; Wnt11+/-
Wnt5a-/-; Wnt11-/-
A
Sox17 DAPI
B
Sox17 DAPI
C
PPH3 DAPI
D
PPH3 DAPI
E
Snail
F
Snail
E'
Snail
F'
Snail

Fig. S10

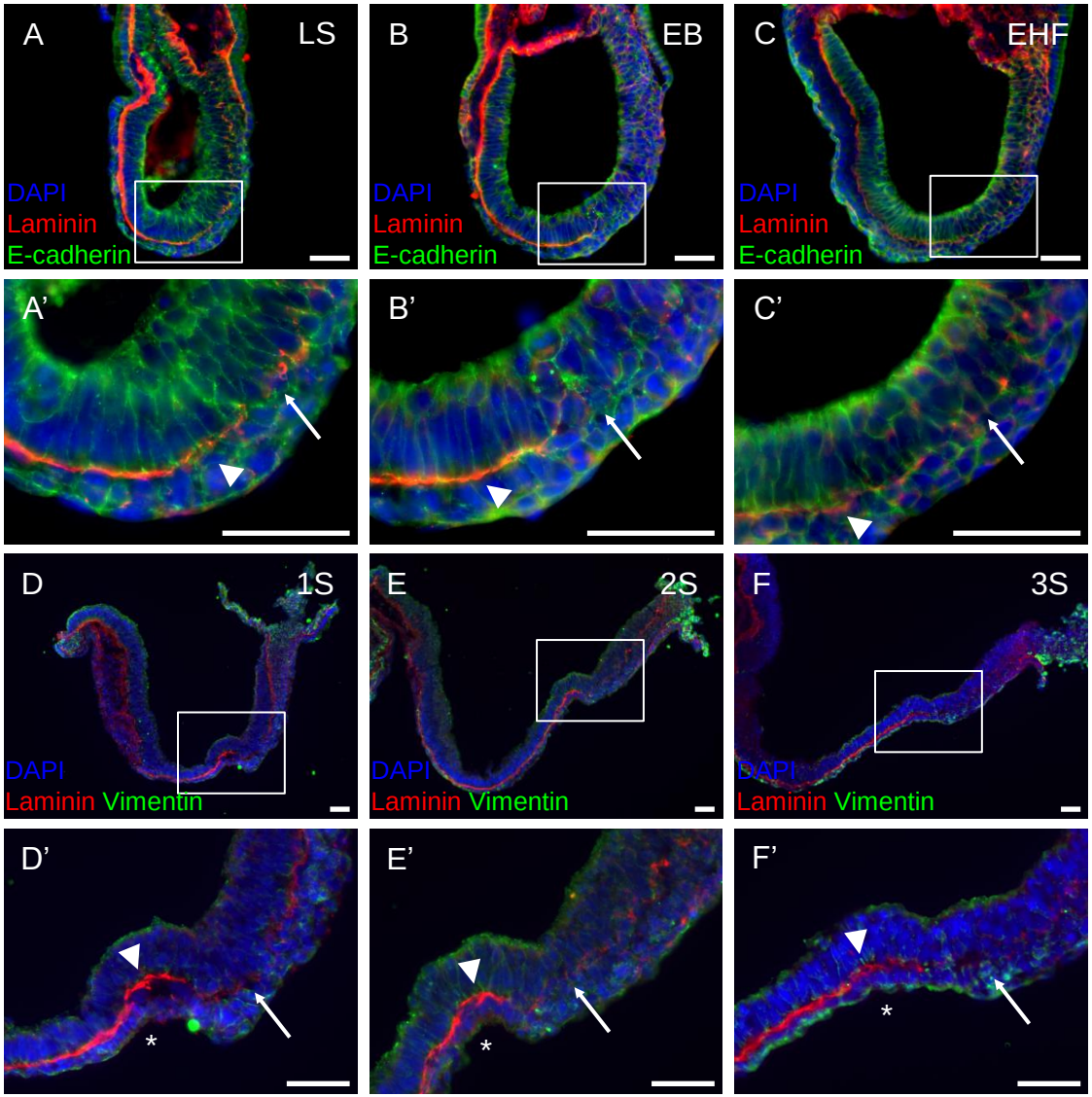
A
LS
DAPI
Laminin
E-cadherin
B
EB
DAPI
Laminin
E-cadherin
C
EHF
DAPI
Laminin
E-cadherin
A'
B'
C'
D
1S
DAPI
Laminin Vimentin
E
2S
DAPI
Laminin Vimentin
F
3S
DAPI
Laminin Vimentin
D'
E'
F'

Fig. S11

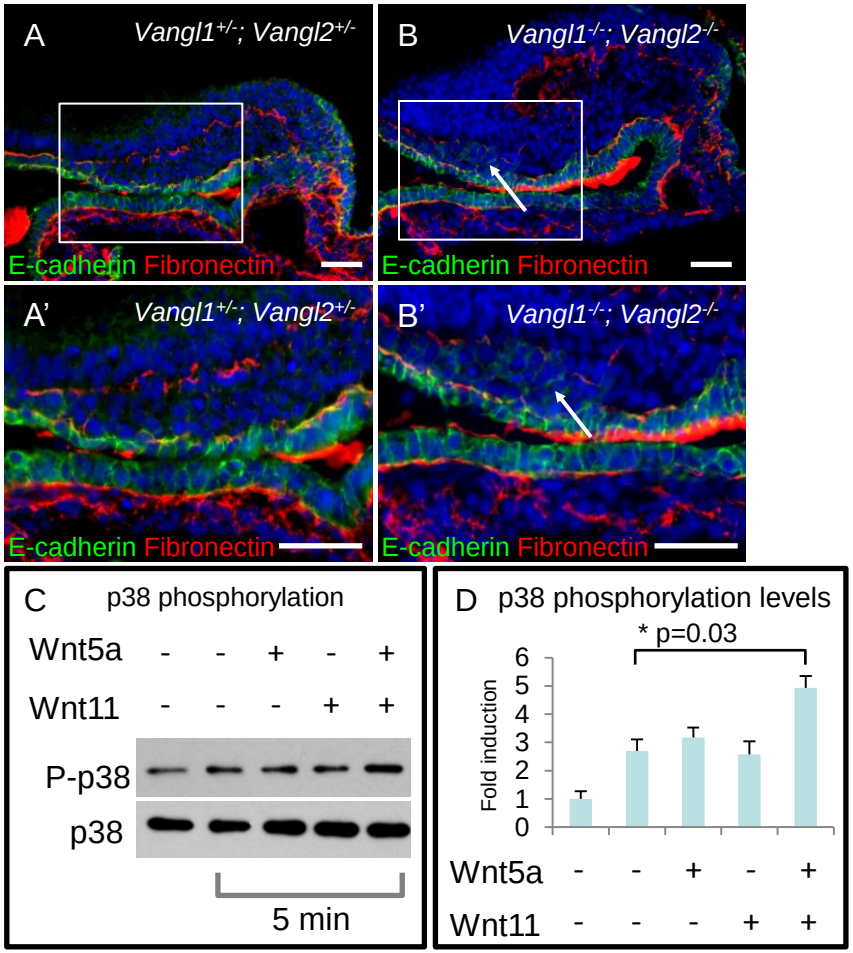
A
Vangl1+/-; Vangl2+/-
E-cadherin Fibronectin
B
Vangl1-/-; Vangl2-/-
E-cadherin Fibronectin
A'
Vangl1+/-; Vangl2+/-
E-cadherin Fibronectin
B'
Vangl1-/-; Vangl2-/-
E-cadherin Fibronectin
C
p38 phosphorylation
Wnt5a - - + - +
Wnt11 - - - + +
P-p38
p38
5 min
D
p38 phosphorylation levels
* p=0.03
Fold induction
0
1
2
3
4
5
6
Wnt5a - - + - +
Wnt11 - - - + +